

Copyright © 2010, Paper 14-004; 79066 words, 14 Figures, 0 Animations, 3 Tables.  
<http://EarthInteractions.org>

# The Influence of Tropical Deforestation on the Northern Hemisphere Climate by Atmospheric Teleconnections

**Peter K. Snyder\***

Department of Soil, Water, and Climate, University of Minnesota, Saint Paul, Minnesota

Received 25 October 2008; accepted 15 February 2010

**ABSTRACT:** Numerous studies have identified the regional-scale climate response to tropical deforestation through changes to water, energy, and momentum fluxes between the land surface and the atmosphere. There has been little research, however, on the role of tropical deforestation on the global climate. Previous studies have focused on the climate response in the extratropics with little analysis of the mechanisms responsible for propagating the signal out of the tropics. A climate modeling study is presented of the physical processes that are important in transmitting a deforestation signal out of the tropics to the Northern Hemisphere extratropics in boreal winter. Using the Community Climate System Model, version 3 Integrated Biosphere Simulator (CCM3-IBIS) climate model and by imposing an exaggerated land surface forcing of complete tropical forest removal, the thermodynamic and dynamical atmospheric response is evaluated regionally within the tropics, globally as the climate signal propagates to the Northern Hemisphere, and then regionally in Eurasia where land-atmosphere feedbacks contribute to amplifying the climate signal and warming the surface and lower troposphere by 1–4 K. Model results indicate that removal of the tropical forests causes weakening of deep tropical convection that excites a Rossby wave train emanating northeastward away from the South American continent. Changes in European storm-track activity

---

\* Corresponding author address: Peter K. Snyder, Department of Soil, Water, and Climate, University of Minnesota, 439 Borlaug Hall, 1991 Upper Buford Circle, Saint Paul, MN 55108.

E-mail address: [pknyder@umn.edu](mailto:pknyder@umn.edu)

cause an intensification and northward shift in the Ferrel cell that leads to anomalous adiabatic warming over a broad region of Eurasia. Regional-scale land–atmosphere feedbacks are found to amplify the warming. While hypothetical, this approach illustrates the atmospheric mechanisms linking the tropics with Eurasia that may otherwise not be detectable with more realistic land-use change simulations.

**KEYWORDS:** Deforestation; Tropics; Teleconnection

## 1. Introduction

Land-use and land-cover change is of increasing concern to scientists as the human population surpasses 6.5 billion people early in the twenty-first century (Foley et al. 2005). More people are dependent on the Earth's limited natural resource base that is already straining under demand. Development pressures add to this problem as land is altered to meet population needs. A large portion of the Earth's surface has already been modified for urban and industrial development, agriculture, and pastureland. Almost 35% of the land surface (nearly 55 million km<sup>2</sup>) has been directly converted to human-dominated systems (Ramankutty and Foley 1999). Of the remaining 65% of the land surface, much is already heavily influenced by human settlement and resource extraction.

The large and ecologically sensitive tropical rain forests of South America, Africa, and Southeast Asia may be most at risk because of population and development pressures (Foley et al. 2007). Annually, over 15 million hectares (ha) (150 000 km<sup>2</sup>) of forests are lost in the tropical rain forests of South America, Africa, and Southeast Asia with 14.2 million ha (142 000 km<sup>2</sup>) converted for other land uses (i.e., pastureland, croplands, etc.) and 1 million ha converted for forest plantations (FAO 2001). A study by Asner et al. (Asner et al. 2005) suggests that previous estimates of forest reduction in the Amazon may be significantly underestimated because of selective logging that is not observable by traditional coarse-resolution satellite measurements. Furthermore, Amazonian forests are increasingly being cleared for cropland, not just for pastureland or timber harvesting, as the demand for energy drives expansion of soybean agriculture for biofuel (Costa et al. 2007).

Although damage to ecological systems and biodiversity is perhaps the greatest threat of expanding land use in the tropical forests, so is the potential for changes to the climate system. Changes in land cover influence how vegetation and soils exchange water, energy, and momentum with the atmosphere through complex biophysical processes (Foley et al. 2003). The resulting changes in the surface energy, water, and momentum balance can affect the thermodynamics and circulation of the atmosphere, thereby altering climate patterns. Such changes in the land surface may strongly affect local and regional climate, but perhaps also the climate of distant locations by atmospheric teleconnections. Although teleconnection processes are well documented in atmospheric research (e.g., Wallace and Gutzler 1981), the focus is often centered on atmosphere-only or ocean–atmosphere processes. Mounting evidence, however, indicates that land-use and land-cover changes may also trigger atmospheric teleconnections. This is an important conclusion because, while it is known that land-use and land-cover changes can strongly impact regional climate, and to a lesser degree, global climate through

spatial averaging of a strong regional climate signal, it is also apparent that a strong and large-scale surface forcing can impact *distant* regions and affect the global climate change signal as well. Although the Intergovernmental Panel on Climate Change (IPCC) acknowledges the contribution of land-use and land-cover changes and their associated land–atmosphere feedbacks on the *regional* climate change signal (e.g., Denman et al. 2007; Hegerl et al. 2007), there is no mention of the contribution of land-use and land-cover changes inducing teleconnection behavior nor discussion of climate model representation of these teleconnection processes.

Tropical landmasses are a large source of energy for the atmosphere and the general circulation is responsible for transporting this energy poleward to maintain the global radiation balance. Consequently, the tropics have a direct influence on the extratropical climate, and any changes to the tropical energy balance and the poleward atmospheric transport processes have the potential to affect the climate at higher latitudes.

In the tropics, one of the ways in which land-use and land-cover change can affect the atmospheric energy is through changes in deep convection. Deep tropical convection, fueled by heat and moisture through the release of latent energy, drives plumes deep into the troposphere and is the main source of precipitation in the tropics. The outflow region of tropical convection occurs around 200 hPa and is characterized by strongly divergent winds responsible for transporting energy poleward. Changes in the spatial position and intensity of these deep convection centers can, however, affect the outflow intensity, poleward transport, and the extratropical climate.

The potential for land use to alter tropical deep convection, high-altitude divergent outflow, poleward energy transport, and extratropical climate has a precedent. Several studies have considered how changes in tropical ocean conditions, especially changes in sea surface temperature that can drive changes in atmospheric heating and deep convection, may affect the tropical circulation regime and their communication to the extratropics (e.g., Hoskins and Karoly 1981; Trenberth et al. 1998). Interestingly, tropical land-use change may initiate heating anomalies and an atmospheric response that are similar to that generated during an El Niño–Southern Oscillation (ENSO) event. The analogy between tropical deforestation (a relatively slow process, occurring over many years and decades) and an El Niño event (a fairly rapid change in ocean conditions, lasting only months to a year or two) should not be stretched too far. Nevertheless, the kinds of teleconnection processes observed between the tropics and the midlatitudes during ENSO events may also be applicable to land-use change studies as detailed in this paper.

There have been many regional-scale studies detailing the effects of deforestation on the tropical climate. A study by Dickinson and Henderson-Sellers (Dickinson and Henderson-Sellers 1988) examined how Amazonian deforestation could affect the local and regional climate when tropical forests were replaced by grasslands. Using a biophysical land surface model coupled to an atmospheric general circulation model (AGCM), they quantified how deforestation changes the aerodynamic roughness and reduces the turbulent mixing of water, energy, and momentum between the surface and the planetary boundary layer. Dickinson and Henderson-Sellers concluded that large-scale deforestation of the Amazon basin could lead to a temperature increase of 3°–5°C and a significant decrease in precipitation. More recent studies have come

to similar conclusions: tropical deforestation causes a regional-scale warming and decreases in regional precipitation and evapotranspiration (Da Silva et al. 2008; Hahmann and Dickinson 1997; Henderson-Sellers et al. 1993; Lean and Warrilow 1989; Lean and Rowntree 1993; Lean and Rowntree 1997; Nobre et al. 1991; Snyder et al. 2004a; Snyder et al. 2004b). A more complete summary of recent tropical deforestation modeling efforts is provided by Costa and Foley (Costa and Foley 2000). Finally, Betts et al. (Betts et al. 2004) describe how large-scale tropical forest dieback could result from biogeophysical feedbacks due to the physiological response of vegetation to elevated CO<sub>2</sub>. Unlike the other studies, they did not explicitly impose land-cover changes; however, the resulting biological behavior produced similar regional results (e.g., warmer and drier) with some larger-scale climate changes that could amplify the dieback.

A handful of studies have also examined how the effects of tropical deforestation may extend beyond the tropics. Henderson-Sellers et al. (Henderson-Sellers et al. 1993) for example, hypothesized that tropical deforestation could induce large-scale circulation changes, including changes to the Walker and Hadley circulations. Another modeling study by Sud et al. (Sud et al. 1996) suggested that tropical deforestation could lead to changes in the meridional circulation of the Southern Hemisphere.

More recently, Gedney and Valdes (Gedney and Valdes 2000) linked deforestation in Amazonia to possible changes in winter rainfall over the northeast Atlantic and western Europe. Using an AGCM, they concluded that anomalous Rossby wave propagation out of the tropics and a reduction in the descending branch of the Hadley cell were primarily responsible for the extratropical climate changes. Avissar and Werth (Avissar and Werth 2005) also investigated the linkage between tropical deforestation and extratropical precipitation changes. Their results indicated that statistically significant precipitation changes occurred when different regions were deforested and replaced with grasses and shrubs; however, the exact cause-and-effect relationship of the dynamical processes leading to these hydroclimatological changes is unclear. A more recent study by Hasler et al. (Hasler et al. 2009) has also explored the influence of tropical deforestation on the extratropical precipitation response using a multimodel ensemble approach. They found a statistically significant signal in precipitation in the tropics but a considerably weaker signal in the extratropics. In addition, the authors found an extratropical dynamical response in the geopotential height field indicating that tropical deforestation may influence planetary wave patterns. Other studies have also indicated that land-use and land-cover change in the tropics may influence the extratropical climate through changes in the general circulation; however, the magnitude of the extratropical response varies (Chase et al. 2000; Pielke 2001; Werth and Avissar 2002; Zhang et al. 1996; Zhao et al. 2001). In contrast, a modeling study by Findell et al. (Findell et al. 2006) found that a tropical deforestation signal is not likely to be detectable from natural climate variability outside of the tropics.

In a comprehensive land-cover change modeling intercomparison project, Pitman et al. (Pitman et al. 2009) used a suite of seven coupled atmosphere–biosphere models to evaluate the regional and global climate response of past land-cover change. Globally, they found no remote impacts related to the observed land-cover change in the set of models; however, as the authors point out, this may be a result of 1) the individual model representation (i.e., parameterization) of land-cover change

and 2) the fact that the land-cover forcing included little tropical land-cover change. The latter is important in that teleconnection behavior is well expressed between the tropics and the extratropics and, as the authors indicate, the exclusion of a tropical land-cover change forcing may be a likely contributor to why remote effects were not observed.

While most of these studies agree that tropical deforestation can potentially induce changes in extratropical climate, they do not agree on the magnitude and location of the changes or the specific physical mechanisms that generate them. This study builds on the work of these past studies by explicitly examining the dynamical and thermodynamical behavior in a conceptual experiment.

In this study, the thermodynamic and dynamical mechanisms linking tropical heating anomalies caused by deforestation with the extratropical climate are explored. To achieve this goal, deforestation simulations were performed with a coupled atmosphere–biosphere model consisting of an AGCM and a detailed land surface–terrestrial ecosystem model. Section 2 of this paper describes the modeling framework used in this study, including details of the simulation design. Section 3 presents an overview of the climate response to pantropical deforestation, including an analysis of the general tropical climate fields. Section 4 details the physical mechanisms responsible for propagating a signal from the tropical climate to the extratropics, while section 5 describes the extratropical climate response to tropical deforestation. A summary of the connections between the general circulation changes to regional-scale climatic impacts and land–atmosphere feedbacks are discussed in section 6. Finally, section 7 summarizes the basic conclusions of the study and identifies potential mechanisms linking tropical land use to the global climate system.

## 2. Model description and simulation design

This section contains a description of the coupled atmosphere–biosphere model, specific details of the simulations performed, and some limitations of the experimental approach.

### 2.1. Model description

The coupled atmosphere–biosphere model Community Climate System Model, version 3 Integrated Biosphere Simulator (CCM3–IBIS) was used for all simulations in this study (Delire et al. 2002). The atmospheric component of the coupled model is CCM3 version 3.2 (Kiehl et al. 1998)—a fully dynamic atmospheric model that supports a variety of horizontal spatial resolutions, 18 vertical levels using a terrain-following hybrid sigma-pressure coordinate system, and a 20-min time step. CCM3 includes a precipitation model that includes both shallow and deep convective schemes, as well as large-scale precipitation estimates.

The CCM3 model has been coupled to the IBIS model version 2.1 (Foley et al. 1996; Kucharik et al. 2000). IBIS is a global model of land surface and terrestrial ecosystem processes that represents the physical, physiological, and ecological processes occurring in vegetation and soils in a coherent way. IBIS simulates land surface processes (energy, momentum, water, and carbon balance), vegetation

phenology (budburst and senescence), and vegetation dynamics (changes in vegetation cover through growth, competition, and mortality). IBIS calculates these processes on a spatial and temporal scale consistent with that of the AGCM spatial and temporal resolutions. IBIS represents vegetation as two layers (taller “trees” and short “shrubs” and “grasses”). An IBIS grid cell can contain one or more plant functional types (PFTs) that together comprise a vegetation biome. Soil is represented with six layers that simulate temperature, water, and ice content to a depth of 4 m. Canopy photosynthesis is realistically modeled using the  $C_3$  and  $C_4$  physiology scheme of Farquhar et al. (Farquhar et al. 1980). Canopy stomatal conductance (Collatz et al. 1991; Collatz et al. 1992) and respiration (Amthor 1984) are also calculated to establish a link between the vegetation and the atmospheric budgets for the exchange of energy and water. Budburst and senescence in the model are determined by climate factors.

The model was run with fixed vegetation distributions so that vegetation structure and biogeography are not allowed to change in response to the climate, although seasonal phenology is dynamically represented [e.g., the seasonal cycle of leaf area index (LAI)]. IBIS uses a prescribed “potential vegetation” distribution representing an estimate of the vegetation that would exist in the absence of anthropogenic land-use change (Ramankutty and Foley 1999). A current approximation of vegetation removal estimates that tropical deforestation has claimed  $\sim 30\%$  of the tropical forest vegetation.

Global patterns of soil texture, an important factor for soil moisture, are defined according to the International Geosphere–Biosphere Programme Data and Information System (IGBP–DIS) global gridded texture database (IGBP–DIS 2000). The variability of the soil texture across the model domain affects the movement of water through the soil and the availability of water to the vegetation.

Analysis of the climate response from changes to the tropical forest biome necessitates discussion of the physical parameters representing the tropical forests as modeled in CCM3–IBIS. Unlike some coupled atmosphere–biosphere models that use specified biome parameters such as LAI or soil albedo, CCM3–IBIS explicitly simulates the canopy LAI and total surface system albedo at specific model time steps. The total canopy albedo is determined by the canopy architecture (upper and lower canopies) and the solar geometry using a two-stream radiative transfer approach. The canopy architecture uses leaf optical properties (as defined by Sellers et al. (Sellers et al. 1986) and Bonan (Bonan 1995) of reflectance and transmittance in the visible and near-infrared wavelengths for the upper and lower canopies in the tropical forest biomes as listed in Table 1. In addition, the soil albedo is dependent on soil texture as specified by the fraction of sand, silt, and clay, as well as the soil wetness. The individual canopy and soil albedos and the fraction vegetation cover of the grid cell are then used to determine the total surface system albedo of the grid cell.

Although the model is run with a fixed vegetation distribution, vegetation phenology does simulate a seasonal cycle in LAI. The upper limit of the LAI is determined by the potential LAI parameters listed in Table 1 and includes the upper canopy values for evergreen and deciduous trees as well as the lower canopy values for shrubs and grasses. The potential LAI represents the upper limit that can exist for the biome; however, factors such as moisture stress may limit LAI values to less than their potential values listed in Table 1.



## 2.2. Simulation design

To determine the potential role that the tropical forest ecosystem has on the climate, two parallel simulations were run representing a control case with potential vegetation cover and a tropical deforestation case. The control simulation used a potential vegetation distribution (with all biomes intact and in their “natural” locations). For the tropical deforestation simulation *all* of the tropical forests on the planet were eliminated: all of the tropical evergreen forest and woodland cells, tropical deciduous forest and woodland cells, and all cells of the mixed forest and woodland class that fall within the northern and southern extent of the tropical forest biome were replaced with bare ground (Figure 1). This scenario greatly exaggerates the current degree of deforestation—both in terms of geographic extent and the severity of the land-cover change (typically forests are replaced with pastures, croplands, or plantations, not bare ground)—but it is meant to represent an upper bound on how tropical deforestation *could* impact the climate system and to help isolate the mechanisms responsible.

Both simulations were run at a spectral resolution of T42 (equivalent to a  $\sim 2.8^\circ$  latitude by  $2.8^\circ$  longitude grid). All atmospheric and most land surface calculations were run at a temporal resolution of 20 min. To isolate the response of the vegetation alone, the simulations were run with climatologically prescribed sea surface temperatures (SSTs) and a fixed atmospheric  $\text{CO}_2$  concentration of 350 ppmv.

Both simulations were run for 40 years of model time with the last 30 years of each run used for averaging. Results presented in this paper are significant at the 95% confidence level using a Student's  $t$  test, unless specified otherwise. The statistical significance was computed independently for the monthly, seasonal, and annual results. Although the  $t$  test is not always adequate for determining significance of differences between two populations in climate modeling studies, the use of climatological SSTs does reduce model internal variability (noise) since this type of surface forcing is repetitive with the annual cycle, and thus there is no accumulated model bias. This results in reasonable statistical independence from year to year.

When using the Student's  $t$  test there is the possibility that a degree of autocorrelation may exist in the time series. To ensure that this was not the case in the simulations presented here, the degrees of freedom were “adjusted” to account for the degree of autocorrelation in the time series in select variables such as the surface temperature, precipitation, and 200-hPa wind and geopotential height fields. The effective sample size is estimated by taking the absolute lag-1 correlation of the time series over each grid point and then adjusting the degrees of freedom according to Zwiers and von Storch (Zwiers and von Storch 1995). Based on the adjusted sample sizes, the adjusted  $t$  test is calculated accordingly. For the select variables used in this study, the difference between the adjusted and nonadjusted  $t$  tests yielded negligible differences. For the sake of simplicity, results from the unadjusted  $t$  test are presented here.

## 2.3. Limitations of the experimental approach

While this extreme tropical deforestation scenario is used to identify the possible mechanisms forcing the regional-scale climate of the extratropics, it is acknowledged that there are some limitations to the design of the study.

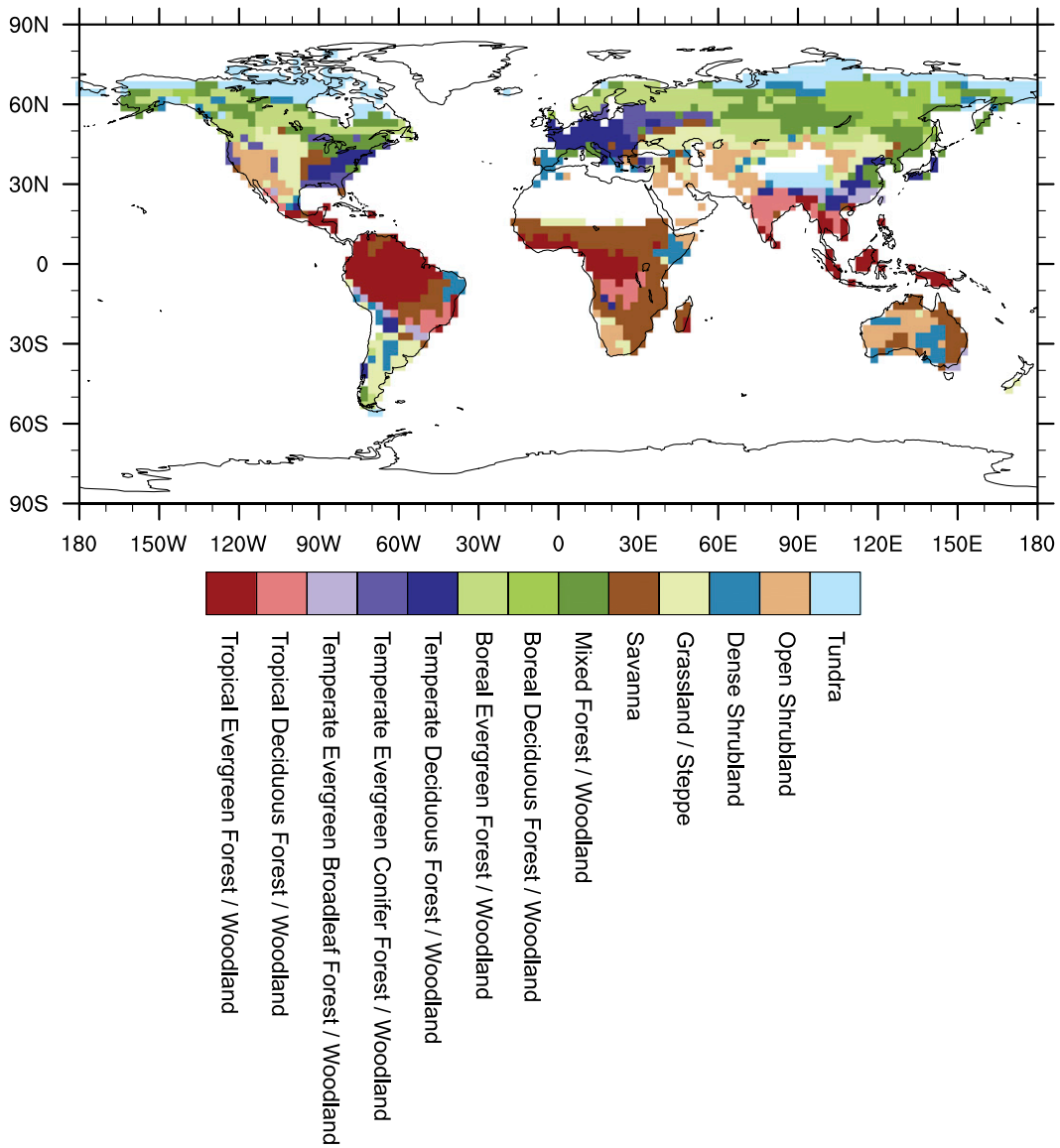


**Figure 1.** Global distribution of potential vegetation used in this study at a spatial resolution of T42. Regions of tropical forest removal include all of the tropical evergreen forest and woodland cells and tropical deciduous forest and woodland cells.

First, while deforestation of the tropics is a very real threat to the environment, the current scale of deforestation does not come close to the area of tropical forest removal used in this study. However, at current deforestation rates, the tropical forests could be mostly cleared by the end of this century (FAO 2001). Regardless, in order to understand the mechanisms forcing the extratropical climate, large-scale and complete deforestation is the best way to ensure that the signal would be “felt” outside the tropics. Certainly, more realistic land-use and land-cover change

could be used to identify current observed climate change as has been discussed in section 1, but many of those approaches do not illuminate the dynamical links between the tropics and extratropics and only identify the cause-and-effect relationship.

Also related to the large-scale deforestation is the limitation of deforesting all three major tropical forest centers (South America, Africa, and Indonesia) simultaneously. Again, while the goal is to identify the important physical processes of tropical–extratropical atmospheric teleconnections, it is possible that deforesting all three tropical regions could potentially affect the Northern Hemisphere general circulation by amplifying the signal from each of the three regions, canceling each continent’s contribution, or a combination of the two. The influence of just one continent or a combination of the three regions, however, might also yield something about the influence of the biome as a whole on the Northern Hemisphere general circulation.

Finally, there are issues associated with using fixed climatological sea surface temperatures in the model. Certainly in the tropics there exist important feedbacks between the continents and the ocean that can mask or amplify the effects of deforestation (e.g., Voltaire and Royer 2005). For instance, it is possible that tropical deforestation could incorrectly estimate the magnitude of the change in the Walker and Hadley circulations because of fixed sea surface temperatures. Fixed sea surface temperatures were required in order to isolate the influence of the vegetation on the climate system alone. Allowing for a dynamical ocean would only increase the complexity in identifying the overall effect of the vegetation on the extratropical climate.

### **3. The climate response to pantropical deforestation**

The overall climate response to tropical deforestation is evaluated by analyzing several climatological fields averaged over the tropical forests of the Amazon basin, Africa, and Southeast Asia, as well as the entire tropical forest biome (Table 2). Results are presented as averages for each season as well as annually. The control run averages for the entire biome are provided for comparison purposes.

Figure 2 shows the simulated seasonal change in global surface air temperatures in response to tropical deforestation. Here the air temperatures increase considerably ( $2^{\circ}$ – $3^{\circ}\text{C}$ ) over parts of all three tropical forest centers for all seasons as evapotranspiration (latent cooling of the surface) is severely reduced with removal of the vegetation. Averaged regionally, Table 2 shows that the large and highly biologically active Amazon region warms the most (by  $\sim 1.8^{\circ}\text{C}$ ) in the September–November (SON) season. The temperature response in Southeast Asia is moderated somewhat by the surrounding ocean, while the large surface cooling in the southern portion of the African tropical forest region is due to regional circulation changes advecting cooler air into the region. The large warming in south-central Siberia and China will be shown in section 5 to be caused by a global teleconnection initiated by tropical forest removal and amplified by changes to the Northern Hemisphere general circulation.

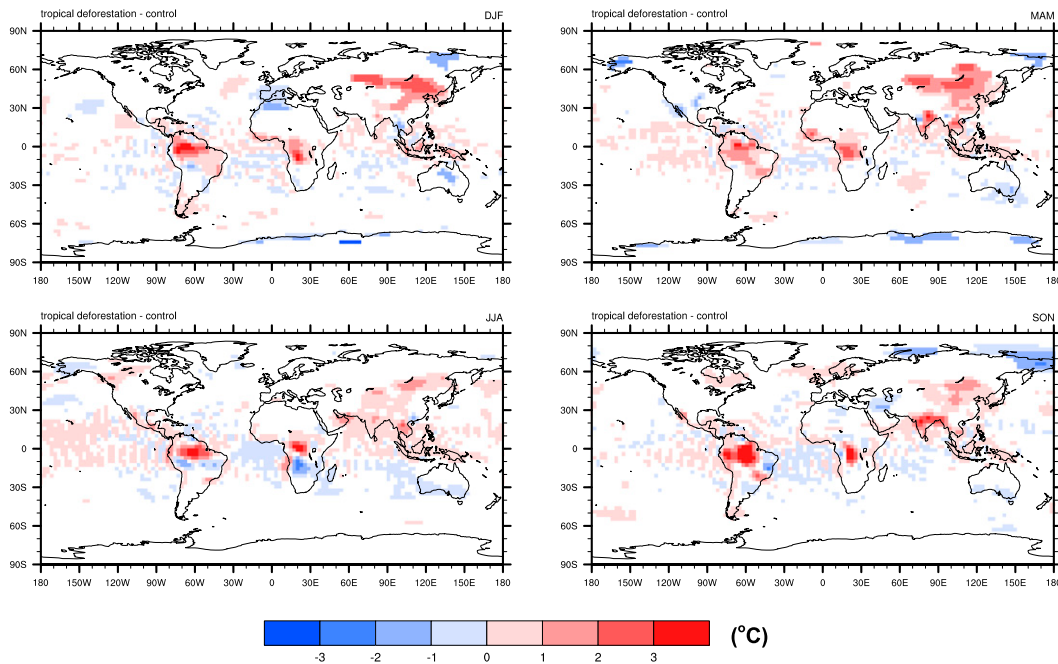
Globally, the tropical rise in temperature with deforestation contributes to a rise in global annual surface temperature of 0.2 or 0.5 K over land areas only (Table 3). Warming in January is greatest (1.3 K globally over land) since this time is when

**Table 2. (a) Selected results from the tropical forest removal simulation. Results are presented as differences (tropical forest removal-control) and averaged annually and seasonally for both individual regions and the entire biome as shown in Figure 1. Averages include only values significant at the 95% significance level using a two-sided Student's *t* test. (b) Seasonal averages may not equal annual averages since locations significant on an annual average may not always be significant for an individual season. All variables shown represent surface-level values except the planetary boundary layer height (PBL height), "total cloud cover," and "high-level cloud cover."**

Variable	(a) Tropical forest removal simulation														
	Amazon basin				Africa				Southeast Asia						
	DJF	MAM	JJA	SON	Annual	DJF	MAM	JJA	SON	Annual	DJF	MAM	JJA	SON	Annual
Temperature (K)	1.2	1.1	0.9	1.8	1.2	1.3	1.4	0.6	1.2	1.0	0.4	0.9	0.8	1.2	0.8
Net radiation ( $W m^{-2}$ )	-15.1	-18.4	-22.6	-27.9	-19.1	-16.6	-14.2	-28.4	-27.1	-19.8	-14.7	-30.0	-12.8	-18.7	-18.1
Albedo (fraction)	0.03	0.04	0.05	0.05	0.04	0.04	0.03	0.07	0.05	0.05	0.04	0.05	0.02	0.03	0.04
Latent heat flux ( $W m^{-2}$ )	-27.7	-29.1	-32.2	-48.8	-30.9	-30.8	-27.5	-33.6	-35.9	-29.6	-20.1	-34.7	-20.8	-30.6	-24.8
Sensible heat flux ( $W m^{-2}$ )	12.7	9.5	10.5	16.4	12.2	12.6	13.7	6.5	9.5	11.6	4.2	1.2	9.3	12.7	6.2
Specific humidity ( $g kg^{-1}$ )	-1.2	-1.3	-1.8	-2.5	-1.7	-1.6	-1.2	-1.8	-1.8	-1.5	-0.7	-1.5	-0.5	-1.5	-0.9
Precipitation ( $mm day^{-1}$ )	-1.5	-1.7	-1.1	-2.5	-1.4	-1.5	-1.0	-1.3	-2.2	-1.2	-1.4	-1.9	-0.3	-1.8	-0.9
PBL height (m)	92.6	92.6	39.4	203.4	109.7	93.2	39.6	43.5	141.9	49.6	-70.6	38.9	11.5	83.4	12.2
Total cloud cover (fraction)	-0.06	-0.07	-0.09	-0.14	-0.08	-0.05	-0.05	-0.07	-0.13	-0.06	-0.01	-0.08	0.00	-0.07	-0.03
High-level cloud (fraction)	-0.08	-0.08	-0.09	-0.14	-0.08	-0.06	0.01	-0.08	-0.14	-0.06	0.00	-0.08	0.02	-0.05	-0.02

Variable	(b) Seasonal averages											
	All tropical				All tropical (control)							
	DJF	MAM	JJA	SON	Annual	DJF	MAM	JJA	SON	Annual		
Temperature (K)	1.0	1.1	0.8	1.5	1.0	296.8	297.8	297.5	298.2	297.6		
Net radiation ( $W m^{-2}$ )	-15.3	-21.1	-21.7	-25.1	-19.0	125.3	135.0	119.1	135.8	128.8		
Albedo (fraction)	0.04	0.04	0.05	0.04	0.04	0.13	0.13	0.13	0.13	0.13		
Latent heat flux ( $W m^{-2}$ )	-26.2	-30.4	-29.6	-40.1	-28.8	104.4	106.0	91.4	110.3	103.0		
Sensible heat flux ( $W m^{-2}$ )	10.3	8.6	9.1	13.7	10.3	22.9	31.0	29.2	27.7	27.7		
Specific humidity ( $g kg^{-1}$ )	-1.2	-1.3	-1.5	-2.1	-1.4	13.8	14.2	13.4	14.5	14.0		
Precipitation ( $mm day^{-1}$ )	-1.5	-1.6	-1.0	-2.3	-1.2	6.0	5.5	4.5	6.5	5.6		
PBL height (m)	45.2	67.3	10.0	158.4	70.0	588.6	646.6	707.3	641.5	646.0		
Total cloud cover (fraction)	-0.05	-0.07	-0.06	-0.12	-0.06	0.74	0.72	0.65	0.76	0.72		
High-level cloud (fraction)	-0.06	-0.06	-0.06	-0.12	-0.06	0.65	0.62	0.52	0.67	0.61		



**Figure 2. Global distribution of seasonal changes in surface temperature (°C) due to tropical forest removal. Differences (tropical forest removal–control) are shown only for cells significant at the 95% significance level using a two-sided Student's *t* test.**

tropical temperature differences are large because of large reductions in latent cooling and the extratropical Asian warming is strongest. The global temperature (not including the tropical forest regions) represents the tropical biome's ability to influence temperatures outside of the region of forcing. In this case, the annual average surface temperature of the globe increases by 0.1 K, or 0.3 K for land areas only. In January, the global temperature of land regions not counting the tropical biome areas is 1.4 K. This large temperature change makes sense when one considers the large area of strong warming throughout Asia as shown in Figure 2.

Figure 3 shows the global precipitation response to tropical deforestation for all seasons. As expected, the precipitation decreases over all three tropical forest regions as reduced evapotranspiration limits the flux of moisture available to the boundary layer. Annual precipitation decreases by 1.2 mm day<sup>-1</sup> when averaged all three regions, while the decrease is largest during the SON season at 2.3 mm day<sup>-1</sup> (Table 2). The large reduction in SON precipitation corresponds to the onset of the wet season as simulated in the model.

While precipitation is greatly reduced over the deforested areas, there are regions within and adjacent to the areas of deforestation where the precipitation increases. The increase in precipitation in the Amazon basin (southern region) in the December–February (DJF) season is likely caused by increased surface convergence of moisture and is consistent with results described by Henderson-Sellers et al. (Henderson-Sellers et al. 1993). Other regions with precipitation increases

**Table 3. Surface air temperature results from the tropical forest removal simulation. Results are presented as differences (tropical forest removal–control) and averaged annually, seasonally, and for January. The regions averaged include the entire globe, only land areas of the globe, the entire globe not including the tropical forest regions, and only land areas not including the tropical forest regions. Statistical significance of results as described in Table 2.**

	DJF	MAM	JJA	SON	Annual	January
Global temperature (K)	0.3	0.4	0.2	0.3	0.2	0.6
Global <sub>land only</sub> temperature (K)	0.7	0.8	0.4	0.7	0.5	1.3
Global (less tropical forest regions) temperature (K)	0.2	0.2	0.1	0.1	0.1	0.5
Global <sub>land only</sub> (less tropical forest regions) temperature (K)	0.5	0.6	0.2	0.2	0.3	1.4

within and adjacent to the deforested areas are caused by regional-scale circulation changes that enhance moisture convergence and increase the energy available for driving tropical convection and possibly influencing the extratropics (Snyder et al. 2004b).

#### 4. The tropical to extratropical forcing mechanism

To begin to explain the Northern Hemisphere climate response to tropical deforestation, and to identify the teleconnection processes at work, it is necessary to methodically track the surface forcing through the atmosphere and to the extratropics. Therefore, this section focuses on the first part of the teleconnection mechanism. That is, the tropical land surface forcing and the atmospheric response followed by the propagation of the signal to the extratropics. Since the tropical-to-extratropical atmosphere linkage is best expressed in Northern Hemisphere winter, here the focus will be on changes to atmosphere and land properties in January.

Convective precipitation dominates in the tropics with much of the precipitation coming from deep convective processes. Deep moist convection is fueled both by heating at the surface (through evapotranspiration and surface warming) and by the release of latent energy through condensation. Deep convective cells can extend upward of 200 hPa to the tropopause where outflow to the extratropics occurs. Deep tropical convection is responsible for initiating the transport of energy out of the tropics and defines the upward branch of the Hadley cell. Therefore, changes to the spatial position and intensity of deep convection can have an impact on the extratropical climate.

Table 2 and Figure 3 show that reductions in precipitation are large throughout the tropics as a result of tropical forest removal. Also shown in Table 2 is the significant reduction in high-level and total cloud cover fraction indicative of reductions in convection.

The effects of tropical forest removal on the high-level outflow can be seen in changes to the 200-hPa velocity potential and divergent wind fields (Figure 4). Through velocity decomposition, the winds at 200 hPa are separated into a non-divergent wind field (rotational) and a divergent wind field (nonrotational). Here, the focus is on the divergent wind field. Figure 4a shows the control run velocity potential and divergent winds at 200 hPa for January. The regions of large positive

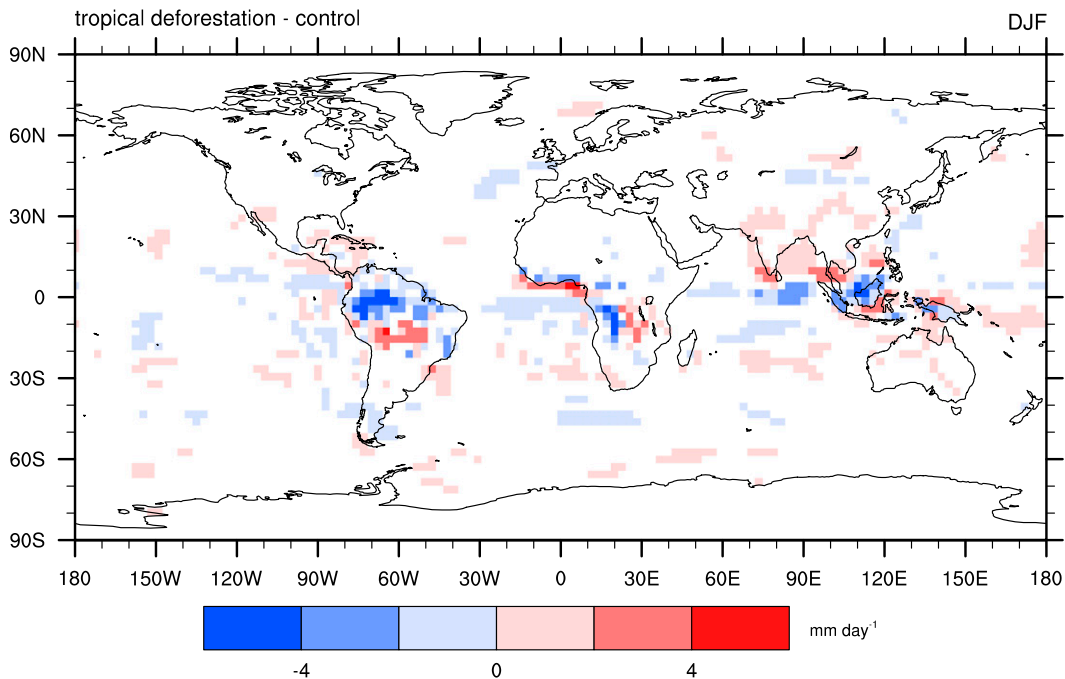


**Figure 3.** Global distribution of seasonal (DJF) changes in precipitation ( $\text{mm day}^{-1}$ ) due to tropical forest removal. Significance of differences as described in Figure 2.

(negative) velocity potential are associated with regions where the divergent winds are strongly diverging (converging). The model accurately captures the divergence out of the tropical forest centers of Africa, Indonesia, and the Amazon and the convergence of the divergent wind field in the extratropics in the regions north and south of the heating centers. After tropical forest removal, the model results indicate that the divergent wind field is weakened over the tropical outflow regions and there is a pronounced weakened convergence located in the vicinity of the East Asian jet and the tropical Pacific region (Figure 4b). Therefore, changes to the tropical outflow (weakened divergent winds) as a result of tropical forest removal and the resulting weakened deep moist convection affect the extratropics through changes to the strength of the Northern Hemisphere westerlies and excite a Rossby wave packet as discussed below.

Changes to the 250-hPa zonal winds are also indicative of the effect that tropical deforestation has on the extratropical circulation. Figure 5 shows the 250-hPa zonal wind field from the control run and the change in the zonal wind field as a result of tropical forest removal. From Figure 5 it is clear that removal of the tropical forests weakens the subtropical westerlies upward of  $6 \text{ m s}^{-1}$ . The 250-hPa zonal winds have the strongest influence on the East Asian jet and, to a lesser degree, the Atlantic jet. Other months of the Northern Hemisphere winter season yield similar responses in terms of changes to the zonal wind intensity from tropical forest removal; however, the exact positioning and intensity of the response appears to

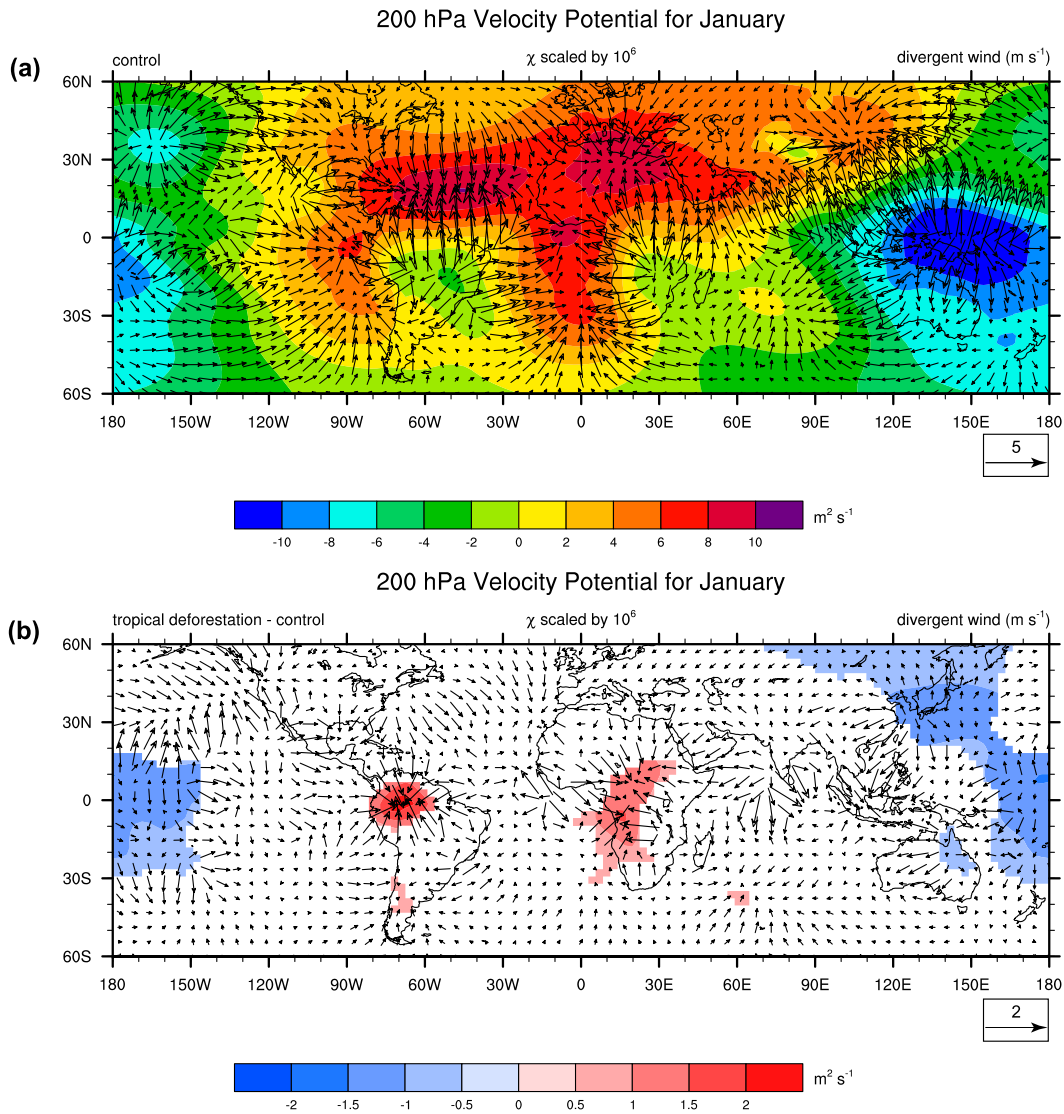


**Figure 4.** Distribution of January 200-hPa velocity potential ( $\text{m}^2 \text{s}^{-1}$ ) and divergent winds ( $\text{m s}^{-1}$ ) for (a) the control simulation and (b) the difference between the tropical forest removal and control simulations. Significance of velocity potential differences as described in Figure 2.

be highly dependent on the different latitudes of the tropical forest regions of Indonesia, Africa, and the Amazon and their contributions to forcing the extratropics at different times.

The high-latitude ( $60^\circ\text{N}$  and  $60^\circ\text{S}$ ) zonal winds (i.e., the polar front jet) are enhanced by  $4\text{--}6 \text{ m s}^{-1}$  across Europe, Asia, the Pacific Ocean, and part of Alaska and are due both to a northward shift and intensification of the zonal winds at that latitude. This dynamical behavior has also been documented by Chase et al. (Chase et al. 2000) in their deforestation modeling study. Enhancement of the high-latitude

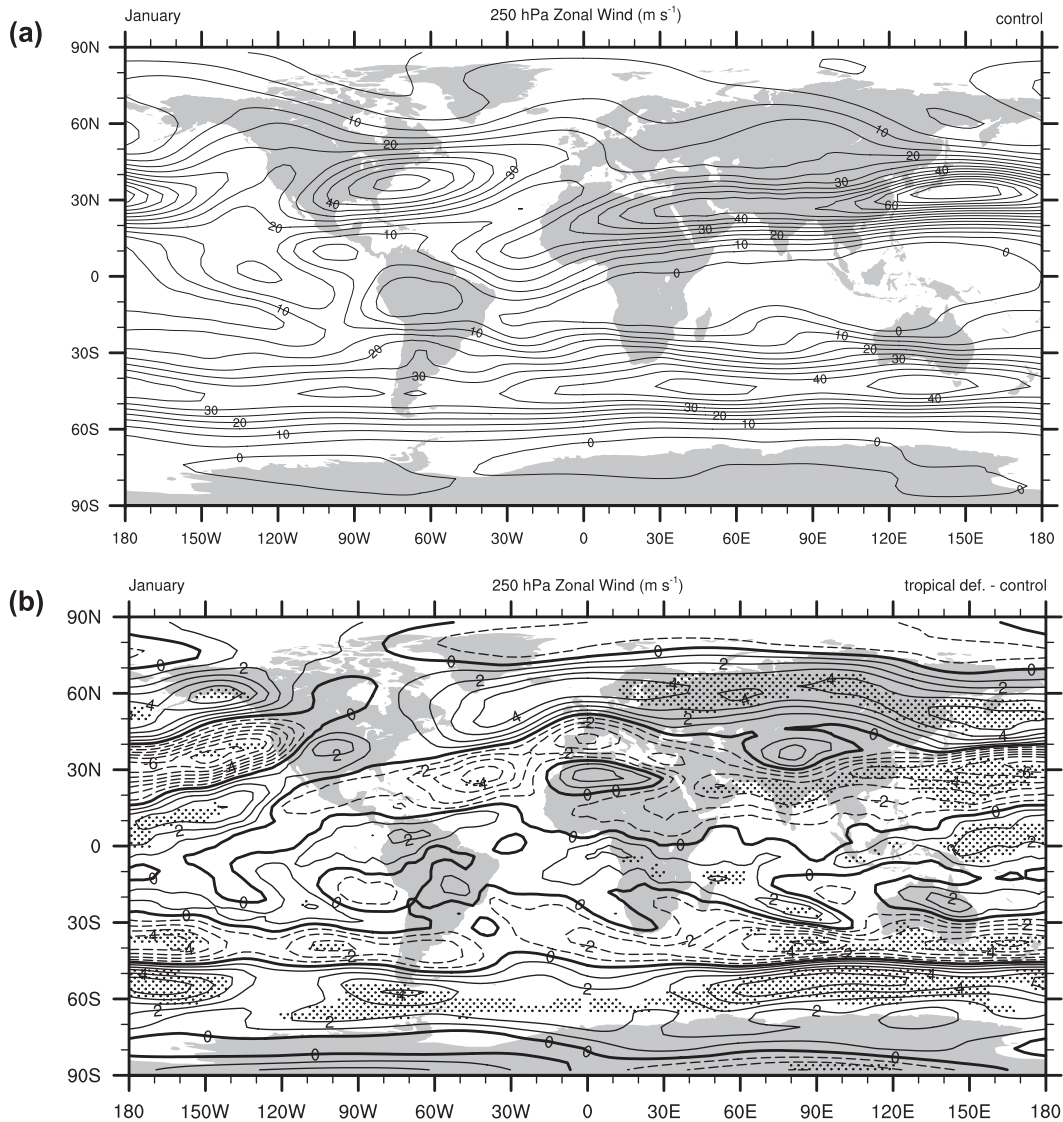


**Figure 5.** Global distribution of January 250-hPa zonal winds ( $\text{m s}^{-1}$ ) for (a) the control simulation and (b) the difference between the tropical forest removal and control simulations. Negative values are indicated by dashed contours and stippling pattern represents statistically significant difference as defined in Figure 2. Contour interval in (a) is  $5 \text{ m s}^{-1}$  and in (b) is  $1 \text{ m s}^{-1}$ .

winds from tropical forest removal may also be an important identifier of changes to an Arctic Oscillation–like behavior.

Analysis of the 250-hPa streamfunction differences between the tropical forest removal and control simulations illustrates how tropical forcing can influence the extratropics through the anomalous forcing of Rossby waves. The mechanism is based on the anomalous vorticity forcing of Rossby waves caused by a weakening

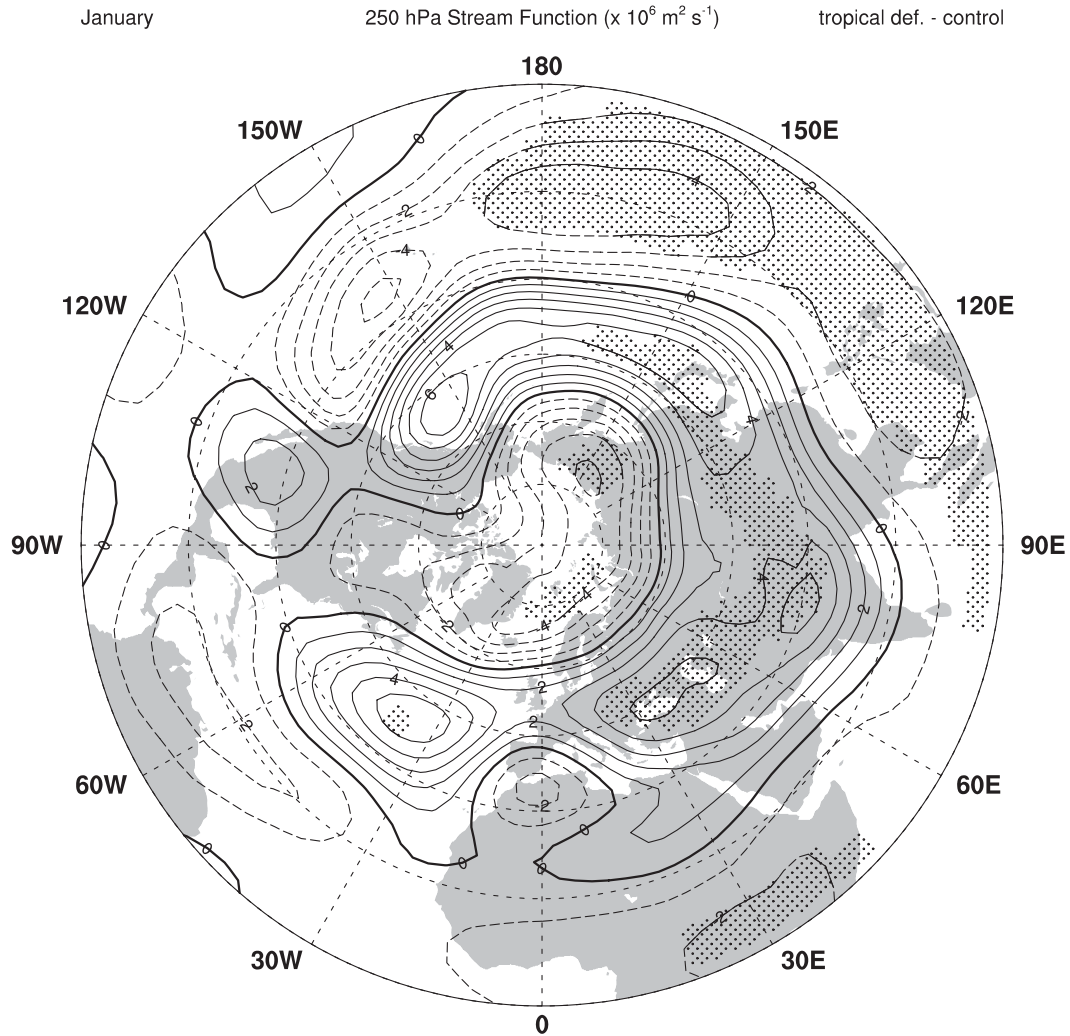


**Figure 6.** Northern Hemisphere changes in the mean 250-hPa streamfunction for January due to removal of the tropical forests. The contour interval is  $10^6 \text{ m}^2 \text{ s}^{-1}$  and negative values are indicated by dashed contours. Stippling pattern represents statistically significant differences as defined in Figure 2.

and repositioning of the centers of tropical outflow, as well as changes to the meridional circulation intensity of the Hadley circulation. Examination of the 250-hPa streamfunction map for January (Figure 6) shows a Rossby wave train emanating from South America ( $\sim 60^\circ\text{W}$ ) and extending north and east across the Atlantic Ocean, Europe, and Asia. The reduction in deep convection stimulated by the land surface forcing excites this anomalous Rossby wave train into northern Europe and Asia. The observed model behavior is remarkably similar to the findings of Gedney and Valdes (Gedney and Valdes 2000) using a form of the European Centre’s Integrated Forecast System AGCM. They found that Rossby wave propagation as

determined from changes in the high-level streamfunction was responsible for influencing precipitation in western Europe. From the results presented here as well as ancillary information from other studies, it is expected that any change to the Northern Hemisphere general circulation is likely forced from changes originating from this tropical location.

While the streamfunction pattern (Figure 6) suggests that the tropical forest region of South America has the largest influence on the extratropics, it is important to note that this pattern is being mildly reinforced by the anomalous outflow from the African and, to a lesser degree, Southeast Asian tropical forests centers as well. However, individual simulations of tropical forest removal for each of the three forest centers indicate that the South American tropical forest center has by far the greatest influence on the regional climate of Eurasia (not shown). Interestingly, the individual continental forest removal results suggest that the extratropical response in the Asian region appears to be a preferred location for climate change both because of the climatological circulation patterns as well as the strong land–atmosphere feedbacks that tend to enhance the signal from the general circulation changes.

Some studies (e.g., Avissar and Werth 2005) have suggested that tropical deforestation, and the Amazon in particular, can have an influence on North American climate; however, the results presented here do not support a North American climate response. This is likely because Rossby wave propagation out of the tropics in the Northern Hemisphere travels northeastward, hence the strong influence on Eurasian climate.

To achieve a North American response, a strong forcing from the tropical forests of Southeast Asia would likely be necessary; however, in these model simulations this is difficult to achieve for two reasons. First, a large percentage of the tropical forestlands in Southeast Asia are located in the Indonesian Archipelago region where the homogeneous area of forested lands are quite small relative to the African and South American tropical forest biomes. Second, and more importantly, the model simulations presented here were run with prescribed climatological sea surface temperatures that are likely to considerably dampen the regional forcing as discussed by Delire et al. (Delire et al. 2001). Using a fully coupled atmosphere–ocean model, Delire et al. found that tropical deforestation of the Indonesian archipelago leads to a reduction in surface roughness and enhancement of near-surface winds, which is in agreement with this study. The authors found that when prescribed sea surface temperatures are used the model tends to enhance the offshore latent heat flux from greater low-level winds and an ocean that is unable to respond by mixing of the thermocline. This behavior is observed in the simulations presented here as the greater moisture flux to the atmosphere enhances precipitation over the ocean regions surrounding the deforested areas in Southeast Asia in all seasons (Figure 3). This contributes to a cooling effect that offsets much of the surface warming due to reduction in evapotranspiration with forest removal. Using a dynamic ocean, Delire et al. found that the increase in near-surface winds enhances equatorial upwelling and mixing of the thermocline such that ocean temperatures decrease and evaporation and precipitation are reduced. They concluded that the climate response to deforestation of the Indonesian archipelago region is likely underestimated in studies that do not use a dynamical ocean configuration. For the results presented here, it is possible that, had a dynamical

ocean been used, a stronger climate response may have been achieved and teleconnection behavior could have resulted in a North American climate response. Further investigation with coupled atmosphere–ocean–biosphere models is needed to dissect the possible contribution of deforestation in this region to the North American and global climate by way of teleconnections.

## 5. Changes to the Northern Hemisphere general circulation

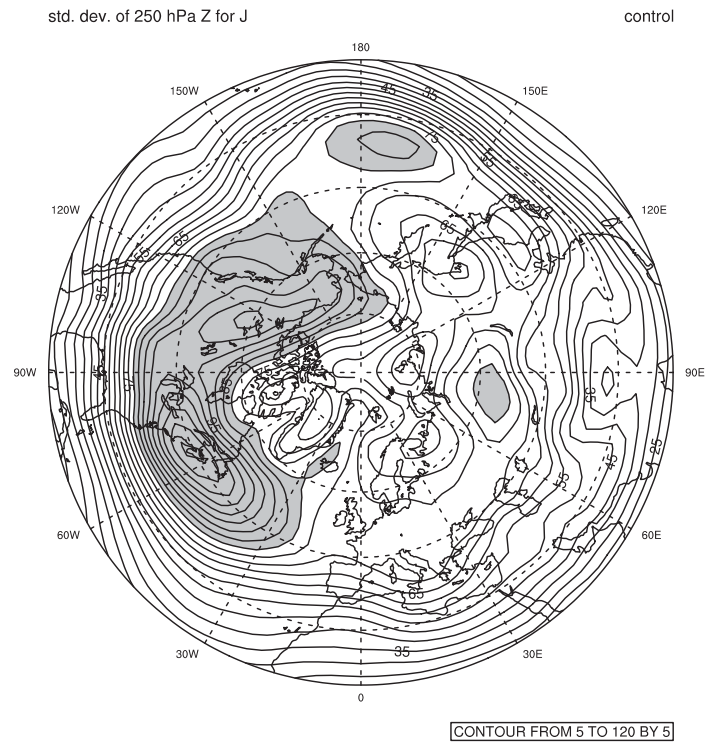
Once the anomalous Rossby wave forcing is in place, changes to the Northern Hemisphere general circulation are made that have an influence on the regional-scale climate in Asia. This section focuses on the second part of the teleconnection mechanism—changes to the general circulation as evidenced by modification of synoptic-scale patterns.

The anomalous forcing of Rossby waves as evidenced by the wave train emanating from just north of the South American continent leads directly into the North Atlantic and northern European region (Figure 6). The large-scale circulation pattern anomalies change the synoptic-scale storm-track positions in the vicinity of northern Europe, northern Asia, and the northeastern part of Asia. Changes to the mean storm tracks are represented in Figure 7 as the standard deviation of the 250-hPa geopotential heights derived from bandpass-filtered (2–8 days) daily data for the control run (Figure 7a) and for the difference between the two runs (Figure 7b). The most notable change is found in the northern European region centered over the Scandinavian countries where there is enhanced storm-track activity with tropical forest removal. Farther east, there is an extended area of increased storm-track activity from Lake Baikal east to the Pacific Ocean. The enhanced storm-track frequency, primarily over the Scandinavian countries, results in anomalous momentum fluxes imparted on the region from transient synoptic-scale eddies as well as anomalous changes to the stationary planetary waves. The anomalous momentum fluxes are also transported downstream of the northern European forcing center where they impact the flow across Asia.

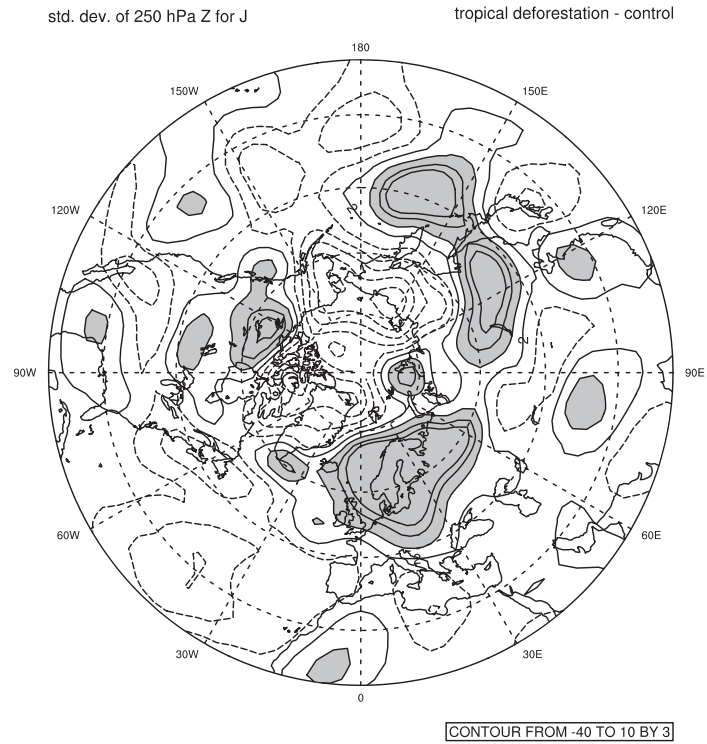
The anomalous eddy momentum flux forcing caused by the variations in the storm track modifies the zonal winds across Europe and Asia. To evaluate how the general circulation changes in this region, the sector average (20°–120°E) zonal wind and eddy momentum flux changes are examined. Figure 8 shows the control and difference for the zonal winds over the European and Asian sector. In general, there is a small weakening of the subtropical jet and intensification (or northward shift) in the polar front jet by more than  $4 \text{ m s}^{-1}$ . This is consistent with the results shown in Figure 5 and is caused by the enhanced eddy momentum flux due to the increase in synoptic-scale eddies. Figure 9 shows the zonal average eddy momentum flux for the control and difference. Of note is the northward shift and intensification in the Northern Hemisphere zonal average eddy momentum flux by more than  $10^\circ$  of latitude and  $4 \text{ m}^2 \text{ s}^{-2}$ . That is, in the tropical forest removal simulation the region of the largest values of the zonal average eddy momentum flux is wider with a pronounced northward shift. The change is much larger in the Southern Hemisphere, although the surface climate response is almost nonexistent because of the small fraction of land area at that latitude.

As the zonal average eddy momentum flux shifts northward (broadens and intensifies) as shown in Figure 9, the vertical gradient of the horizontal eddy

(a)



(b)



momentum flux also changes. Using a conventional Eulerian mean approach, we know that large-scale fluxes of eddy heat and momentum are responsible for driving an indirect mean meridional circulation (i.e., the Ferrel cell). The indirect meridional circulation is a result of eddy fluxes causing changes in the zonal wind and temperature fields. The pressure gradient force that results from changes in the mean zonal wind from geostrophic balance causes an indirect mean meridional circulation to develop, which is necessary to adjust the mean zonal wind and temperature fields such that thermal wind balance is maintained. This behavior is captured in the model simulations of tropical deforestation.

Simulation results show that removal of the tropical forest biome alters the eddy momentum flux more than the eddy heat flux, although both are responsible for altering the mean meridional circulation. Given that the mean meridional circulation due to the large-scale horizontal eddy momentum flux is defined as

$$\bar{X} \propto \frac{\partial^2}{\partial y \partial z} (\text{large - scale eddy momentum flux}),$$

where  $\bar{X}$  is the mean meridional streamfunction; this means that the eddy momentum flux convergence as represented by

$$\frac{\partial^2 \overline{u'v'}}{\partial y \partial z} < 0$$

will be positive and increasing with height north of 30° latitude in the troposphere. This produces the thermally indirect eddy-driven mean meridional circulation (Ferrel) cell. This behavior is summarized in the cartoon in Figure 10. The Coriolis force of this induced indirect meridional circulation is required to balance the acceleration due to the momentum flux convergence; otherwise, the flux convergence would increase the vertical shear of the mean zonal wind and destroy the thermal wind balance.

Changes in the eddy momentum flux convergence influence the position of the Ferrel cell in the simulation due to changes to the meridional and vertical gradient of the eddy momentum flux. These changes modify the meridional position of the descending branch of the Ferrel cell by shifting it northward. This repositioned

---

←

**Figure 7. Northern Hemisphere distribution of the January standard deviation of the 250-hPa geopotential heights (m) for (a) the control simulation and (b) the difference between the tropical forest removal and control simulations. Standard deviations are derived from bandpass filtered (2–8 days) daily data and represent the mean storm tracks. Contour interval in (a) is 5 m and in (b) is 3 m. Shading in (a) represents values greater than 80 m and in (b) values greater than 5 m.**

---

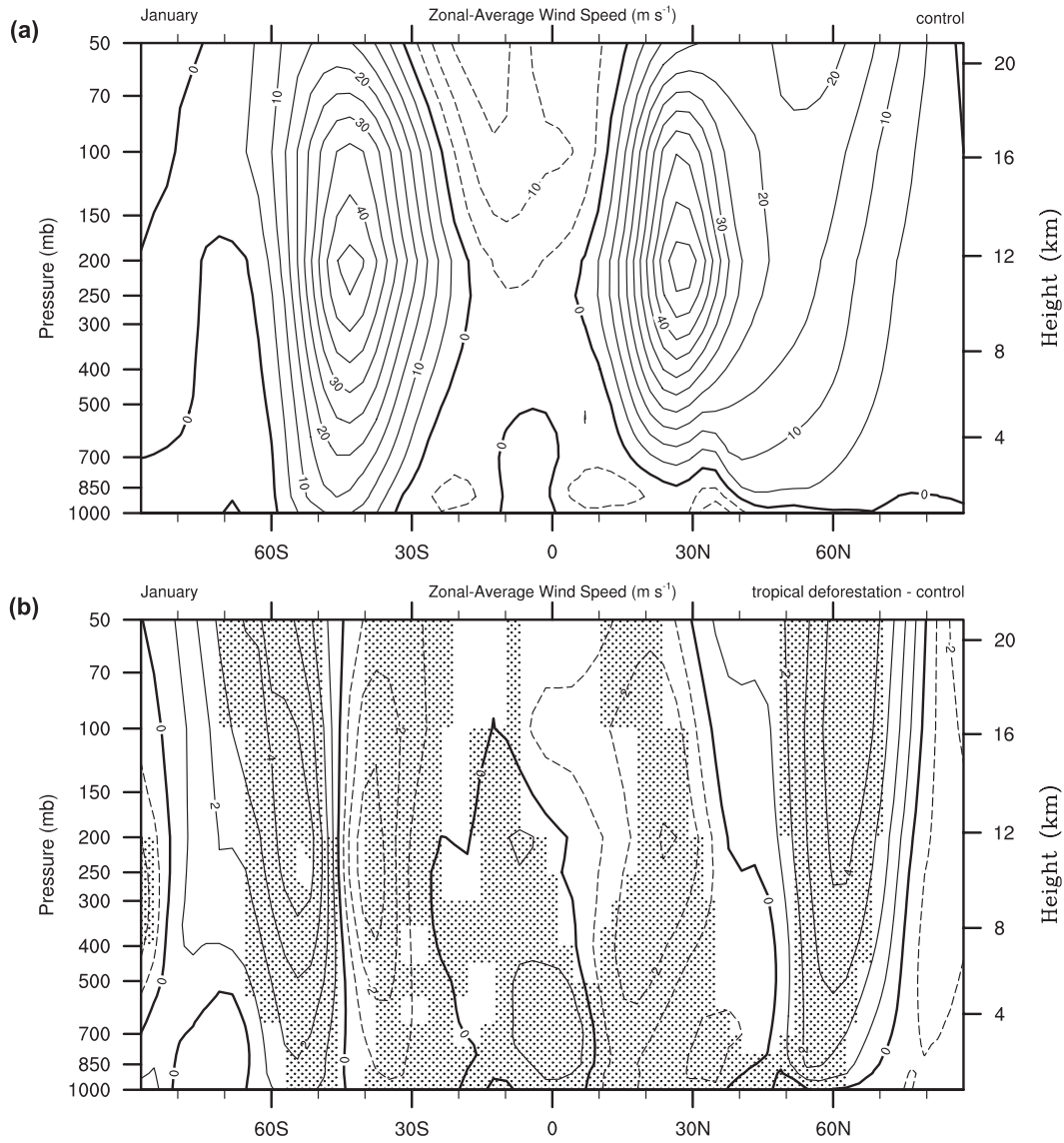


**Figure 8.** Sector average (20°–120°E) distribution of the January zonal winds ( $\text{m s}^{-1}$ ) for (a) the control simulation and (b) the difference between the tropical forest removal and control simulations. Negative values are indicated by dashed contours and stippling pattern represents statistically significant difference as defined in Figure 2. Contour interval in (a) is  $5 \text{ m s}^{-1}$  and in (b) is  $1 \text{ m s}^{-1}$ .

descending branch of the cell results in enhanced adiabatic warming along a latitude band centered on  $\sim 50^\circ\text{N}$  in the European–Asian sector (Figure 11). The warming extends upward into the lower troposphere to heights greater than 800 hPa, although warming is greatest near the surface where land–atmosphere feedbacks amplify the warming.

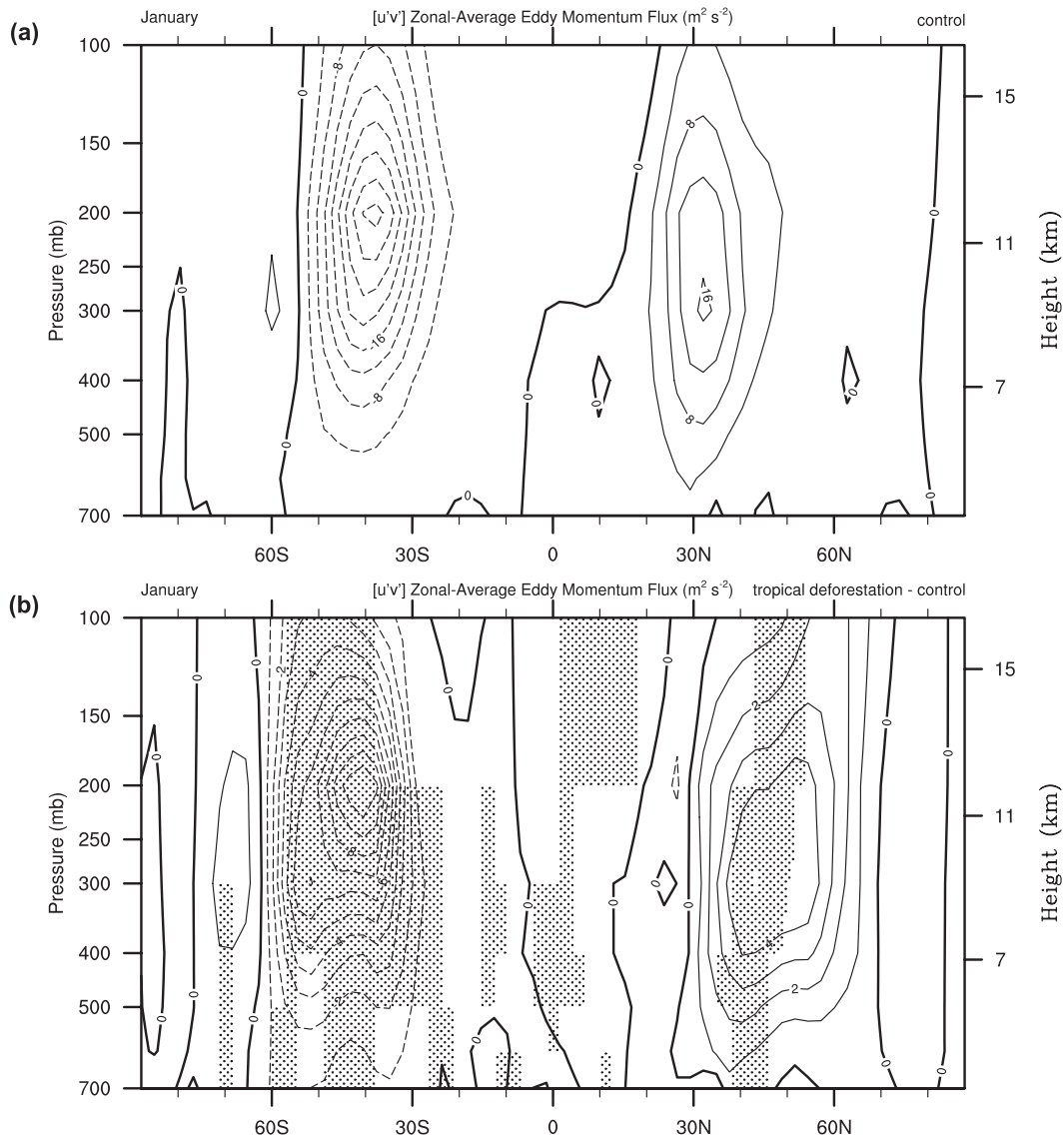


**Figure 9.** Sector average (20°–120°E) distribution of the January eddy momentum flux ( $\text{m}^2 \text{s}^{-2}$ ) for (a) the control simulation and (b) the difference between the tropical forest removal and control simulations. Flux values based on bandpass-filtered (2–8 days) daily data. Negative values are indicated by dashed contours and stippling pattern represents statistically significant difference as defined in Figure 2. Contour interval in (a) is  $4 \text{ m}^2 \text{ s}^{-2}$  and in (b) is  $1 \text{ m}^2 \text{ s}^{-2}$ .

## 6. Regional-scale land–atmosphere feedbacks in the extratropics

Once the northward shift in the descending branch of the thermally indirect Ferrel cell occurs, the enhanced adiabatic warming combined with regional-scale

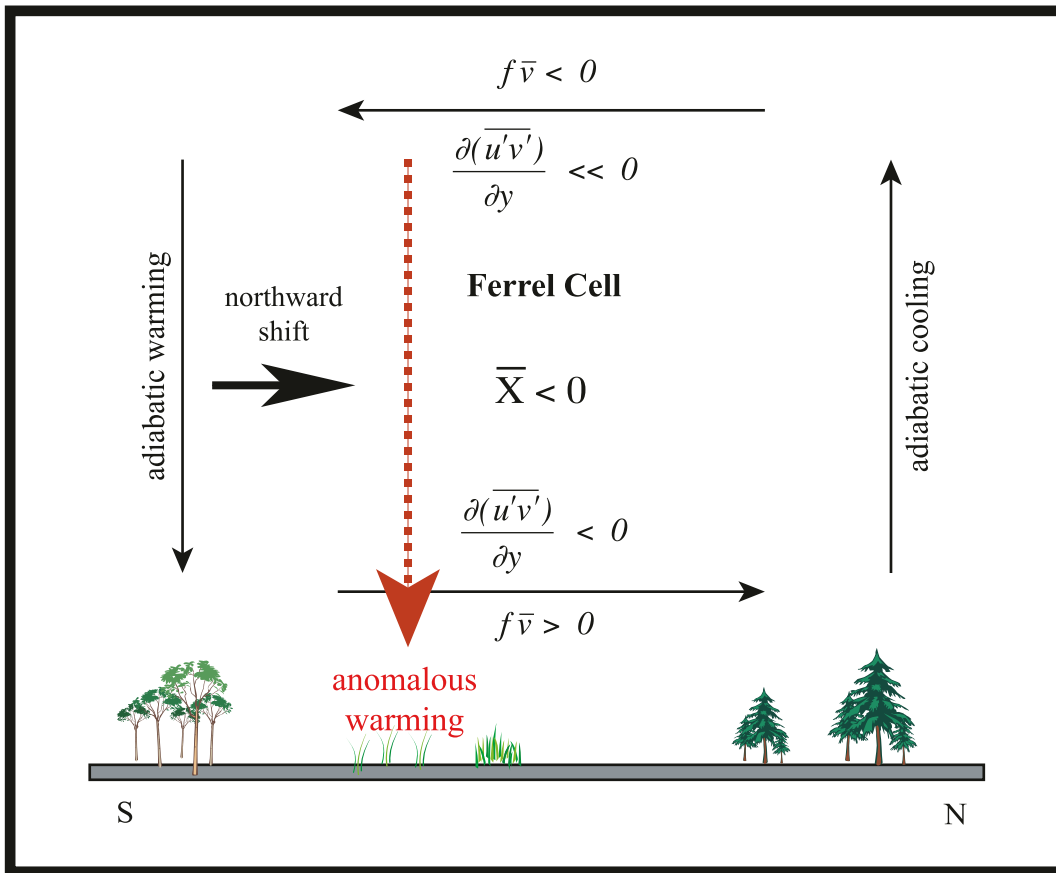


**Figure 10.** Illustration of the relevant components of the midlatitude Eulerian mean meridional circulation forced by a vertical gradient in eddy momentum flux convergence. The anomalous warming presented here is related to the northward shift in the descending branch of the Ferrel cell and is driven by the corresponding shift in the large-scale eddy momentum flux due to removal of the tropical forests.

land–atmosphere feedbacks are initiated that act to increase the temperature of the lower troposphere and land surface (Figure 11).

An increase in the lower-tropospheric temperature increases the height of the planetary boundary layer and decreases the fraction of low-level cloud cover (Figure 12a). Although January is a time when the Northern Hemisphere high latitudes are receiving a minimum of solar radiation, the latitude at which the Ferrel cell is anomalously shifted northward and where the warming is occurring is still at a low enough latitude such that incoming solar radiation is influential in affecting the regional-scale climate. The reduction in low-level cloud cover fraction increases the amount of net radiation absorbed at the surface. The increased net radiation at the surface contributes to snowmelt (not shown) and leads to a decrease in the surface albedo by 0.2 to 0.3 (Figure 12b). This acts as a positive feedback since the lower surface albedo further increases the amount of net radiation absorbed at the

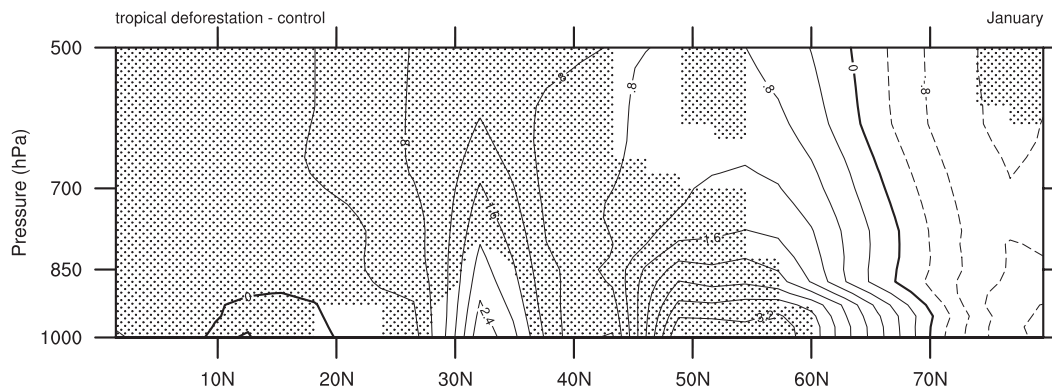


**Figure 11.** Sector average (20°–120°E) distribution of the January changes in temperature (K) between the tropical forest removal and control simulations. Stippling pattern represents statistically significant differences as described in Figure 2. Contour interval is 0.4 K.

surface. Excess energy is then used to warm the land surface and the boundary layer (Figure 13), most strongly in January.

## 7. Summary and conclusions

While attention has focused on how increases in greenhouse gas concentrations may affect the Earth’s climate, the climate system may also be impacted by changes in land cover, whether natural or anthropogenic (Foley et al. 2003; Foley et al. 2005; Pielke et al. 2002). Numerous studies have indicated that tropical deforestation can have a profound impact on the climate of tropical landmasses, and some recent studies have also indicated that these may spread into the extratropics (Avissar and Werth 2005; Chase et al. 2000; Findell et al. 2006; Gedney and Valdes 2000; Hasler et al. 2009; Henderson-Sellers et al. 1993; Pielke 2001; Polcher 1995; Snyder et al. 2004a; Snyder et al. 2004b; Sud et al. 1988; Sud et al. 1996; Werth and Avissar 2002; Zhang et al. 1996; Zhao et al. 2001). The detailed physical mechanisms linking tropical deforestation to extratropical climate changes, however, are still not completely understood primarily because the realistic land surface changes imposed are too weak to be clearly detected by examination of dynamical changes.

Because the tropics are an important source of energy for the extratropical atmosphere, changes in the thermodynamics and dynamics of the tropical atmosphere can often be felt around the globe. In the tropics, the anomalous forcing of Rossby waves can have a direct impact on the Northern Hemisphere general circulation and climate through atmospheric teleconnections. This study confirms the role of planetary wave forcing in communication of a tropical signal to the extratropics and is in agreement with the study by Gedney and Valdes (Gedney and Valdes 2000). This study also indicates that the Eurasian climate response is most likely caused by changes in the Amazon and that the Amazon has little influence outside of Eurasia as suggested by other studies.

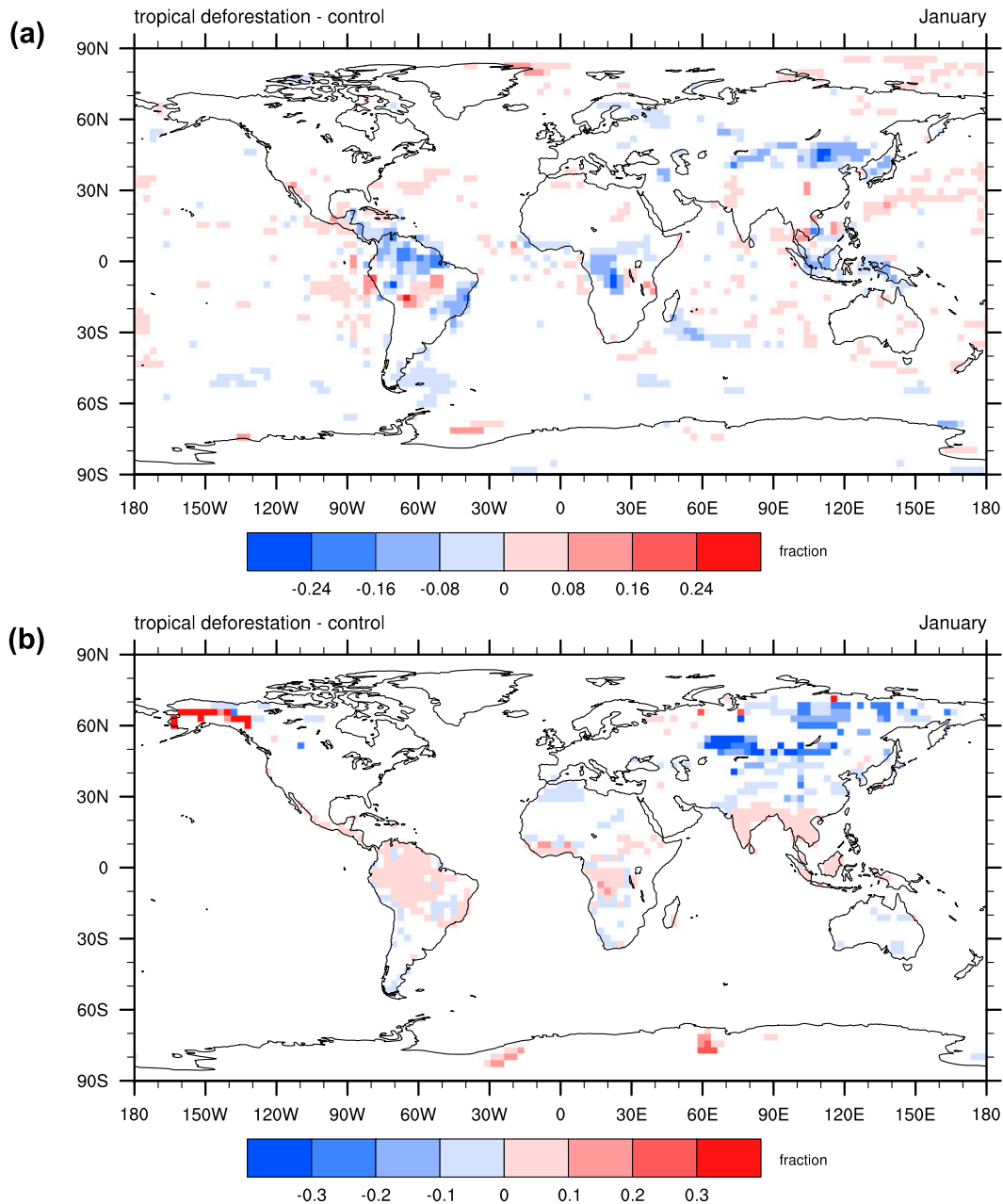


**Figure 12.** Global distribution of January changes in (a) low-level cloud cover (fraction) and (b) land surface albedo (fraction) due to tropical forest removal. Significance of differences as described in Figure 2.

In this paper it has been shown how tropical deforestation *could* affect the extratropical climate and that deforestation influences not only the regional climate of tropical continents through reductions in the latent heat flux, moisture flux, and net radiation, but also the extratropics through a large reduction in deep moist convection and general circulation changes. The extratropical response was found

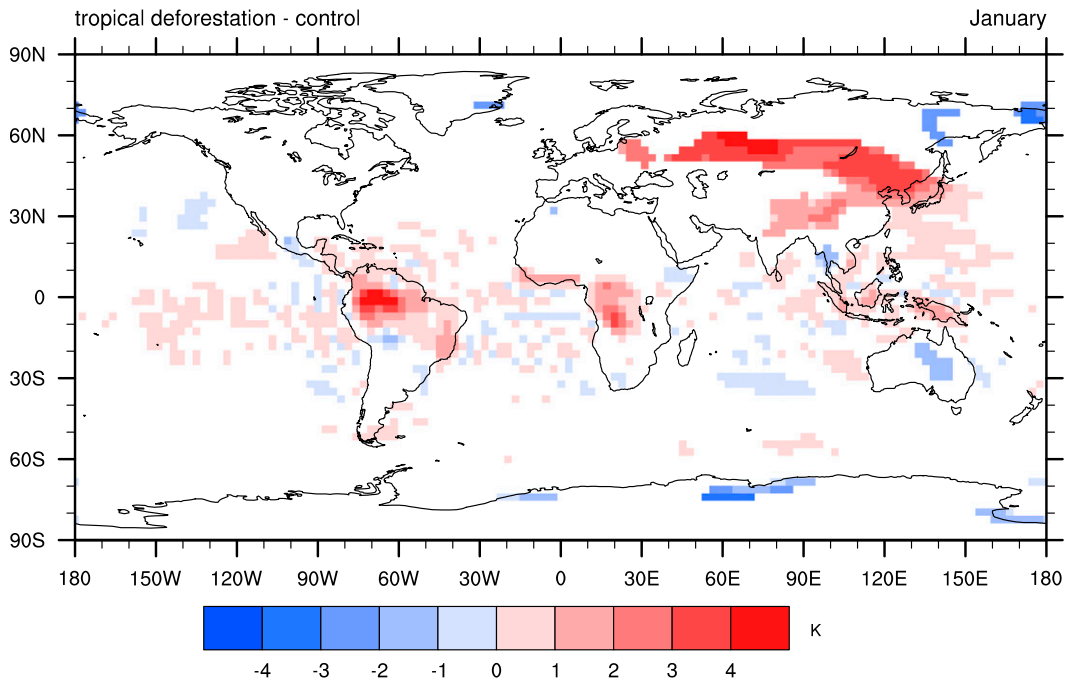


**Figure 13.** Global distribution of January changes in surface temperature (K) due to tropical forest removal. Significance of differences as described in Figure 2.

to be strongest across Eurasia in Northern Hemisphere winter and to a lesser extent the spring; however, the temperature anomalies from tropical forest removal exist throughout the year (see Figure 2).

Decreasing deep tropical convection affects the high-level outflow of energy from the tropics to the extratropics. Divergence at  $\sim 200$  hPa is significantly reduced after deforestation as there is less energy available from the surface to drive deep moist convection. This leads to an anomalous forcing of planetary waves as evidenced by a Rossby wave train emanating from the north of the South American continent to the northeast into western Europe. Changes in the winter storm track lead to modification of the climatological eddy momentum fluxes and repositioning of the thermally indirect mean meridional circulation. This results in a northward shift in the descending branch of the Ferrel cell that enhances adiabatic warming from the surface to the midtroposphere. Regional-scale land-atmosphere feedbacks amplify the warming beyond that initiated by changes in the Ferrel cell as is evidenced by reductions in cloud cover, snow cover, and surface albedo that all lead to an increase in net radiation absorbed at the surface. The excess energy at the surface contributes to a broad region of warming.

While it has been demonstrated that tropical deforestation can affect the extratropics in terms of regional warming in Eurasia, model results also suggest that tropical deforestation can influence the extratropical general circulation in other ways. Model results show that with deforestation there is a deepening (decrease) in Northern Hemisphere polar sea level pressure with lower geopotential heights

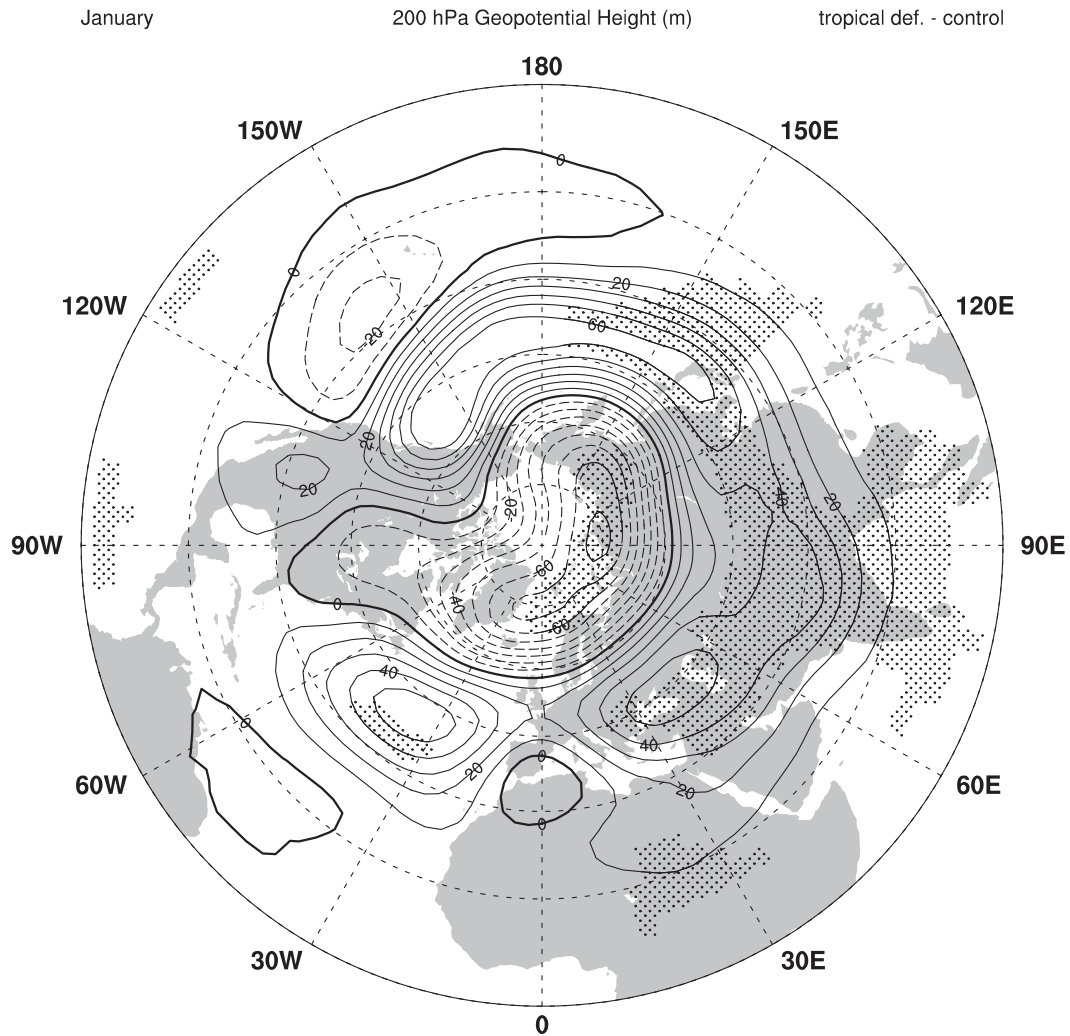


**Figure 14.** Northern Hemisphere changes in the mean 200-hPa geopotential height (m) for January due to removal of the tropical forests. The contour interval is 10 m and negative values are indicated by dashed contours. Stippling pattern represents statistically significant differences as defined in Figure 2.

while a thickening of the troposphere (i.e., increase in geopotential heights) south of 60°N is present (Figure 14). The annular pattern seen in the change of geopotential height as well as changes to the high-latitude jet (Figures 5b and 8b) is *similar* in appearance to the Arctic Oscillation (AO) (Thompson and Wallace 1998; Thompson and Wallace 2000). Although the Arctic Oscillation is more pronounced in the stratosphere at the ~50-hPa height, the annular mode of the circulation at 200 hPa is suggestive of a flow regime that contributes to enhancing the stratospheric polar jet by increasing the upper-tropospheric pressure gradient. This enhanced annular flow prevents cold air from leaving the Arctic at low levels and, on average, enhances southerly flow and warm air advection.

The findings presented here are partially in agreement with other studies exploring teleconnections resulting from tropical deforestation; however, most of these studies have focused on a precipitation, not temperature, response and so direct comparison is difficult. Regardless, a brief summary of these studies and comparison to this study is warranted.

The study by Gedney and Valdes (Gedney and Valdes 2000) most closely resembles the Rossby wave propagation observed in the simulation results presented here. Gedney and Valdes used the 12r1 version of the European Center's Integrated Forecast System GCM at a spectral resolution of T42 ( $2.8^\circ \times 2.8^\circ$ ), 19 vertical levels, and with fixed climatological SSTs. Converting tropical rain forest to grassland in the Amazon led to an increase in surface albedo, reduced surface roughness and fraction cover, and a decrease in LAI. They found a detectable reduction in precipitation, evaporation, net surface radiation and a surface warming of  $1.3^\circ\text{C}$  in the Amazon, which is similar to the response found in this study (Table 2 and Figures 2 and 3). Their results also indicated a northeastward propagation of Rossby waves to the northeast Atlantic and Europe, which is consistent with the behavior identified in the model results (e.g., Figures 6 and 7), and detectable changes in precipitation over Europe. In this study, however, no appreciable precipitation changes were found outside of the tropics (Figure 3).

The studies by Werth and Avissar (Werth and Avissar 2002) and Avissar and Werth (Avissar and Werth 2005) also examined the extratropical precipitation response to tropical deforestation. Both these studies used the National Aeronautics and Space Administration (NASA) Goddard Institute for Space Studies (GISS) GCM 2 model with a spatial resolution of  $4^\circ$  by  $5^\circ$  and 12 vertical levels. The model was run with fixed climatological SSTs and tropical deforestation was represented by conversion of tropical forest to shrubland and grassland. This resulted in an associated increase in surface albedo from 0.06 to 0.1, reduced surface roughness, and a reduction in LAI from 6.0 to 1.0. Their results identified significant extratropical precipitation changes related to either deforestation of the Amazon (as in Werth and Avissar 2002) or the individual tropical forest centers of the Amazon, Africa, and Southeast Asia (as in Avissar and Werth 2005). Although the focus of these two studies was on detection of an extratropical precipitation response and not a dynamical analysis of the atmospheric behavior, a plausible teleconnection mechanism was posited that is in general agreement with the modeled behavior described in this study.

The study by Findell et al. (Findell et al. 2006) used the Geophysical Fluid Dynamics Laboratory atmosphere–land model version 2 at a spatial resolution of  $2^\circ$  by  $2.5^\circ$ , 24 vertical levels, and a slab ocean model to investigate the extratropical climate response to total tropical deforestation. In their simulations, the broadleaf evergreen tropical forests of South America, central Africa, and Oceania were replaced with grasslands. They found an increase in the surface albedo from 0.149 to 0.182 and a decrease in the surface roughness as expected with deforestation. They determined that deforestation leads to a reduction in latent cooling and an annual surface warming of  $1^\circ$ – $3^\circ\text{C}$  in the tropics. Unlike the other studies, they identified little to no extratropical climate response in their model results that would be detectable over natural climate variability. It is unclear why their model shows no extratropical changes while this and other studies do; however, specific model parameterizations may be a contributing factor. Furthermore, Findell et al. used a

slab ocean model rather than fixed SSTs, so this may have played a role in the differences and highlights the need for further insight into the role of atmosphere–ocean–biosphere processes in tropical deforestation studies.

The multimodel study by Hasler et al. (Hasler et al. 2009) also identified a remote response in the precipitation field as well as some changes in the dynamical behavior of the extratropical flow pattern. As with the Werth and Avissar (Werth and Avissar 2002) and Avissar and Werth (Avissar and Werth 2005) studies, tropical forests were replaced with grasses and shrubs. Observed sea surface temperatures were used and run at a spatial resolution of 4° by 5° and either 12 or 26 vertical levels depending on the model. While the results presented here do not show a clear extratropical precipitation response, there is some comparison with Hasler et al. (Hasler et al. 2009) in terms of the dynamical wave pattern changes in the winter and early spring general circulation.

The model intercomparison study by Pitman et al. (Pitman et al. 2009) included analysis of the regional and global response to observed land-cover change in seven atmosphere–biosphere models. The statistical and methodological approach used in their study is similar to the methodology described herein. They found no remote climate changes due to observed land-cover change as identified in this and other studies; however, direct comparison of the results is difficult since they imposed observed land-cover changes that included little in the way of tropical changes. Tropical land-cover changes are likely to produce some of the strongest teleconnection behavior given the Earth's equator-to-pole flow of energy. In addition, the land-cover changes imposed in this study are not based on observed changes, but rather extreme deforestation is used to achieve a strong and clear climate response so as to highlight the dynamical and thermodynamical mechanisms. Importantly, Pitman et al. (Pitman et al. 2009) identified the need for a more rigorous model methodology, statistical testing with multiple models and realizations, and consideration of land-cover forcing in individual models to fully explore the remote climate effects of land-cover change.

While the surface forcing used in this study is more extreme than the studies summarized above (i.e., tropical forest converted to bare ground), the tropical surface response was found in most cases to be similar. So why then do some models show an extratropical response while others do not? The answer could lie in such details as the model setup (e.g., how deforestation is represented), model parameterization (e.g., vegetation model specifics, boundary layer and convective parameterizations), use of fixed SSTs versus a slab or fully dynamical ocean model, or statistical rigor employed on the model output. To better understand whether tropical deforestation has the potential to produce an extratropical climate response will likely require a multimodel intercomparison effort using different models with a similar model setup and statistically analyzed using the same methodology. In addition, the occurrence of statistically significant teleconnection behavior in a model or suite of models is not in itself sufficient. There must also be a coherent explanation of the mechanisms leading to the change that is consistent with our understanding of atmospheric physics. This study has both identified teleconnection behavior and described the mechanisms.

While the specific results of this study need additional confirmation, it is now clear that a dynamical mechanism is in place for explaining how tropical deforestation can have global climatic effects. Few studies have identified how this

might be possible, but here it has been illustrated that there can be a physical mechanism whereby tropical deforestation forcing is communicated to the extratropics through explainable teleconnection mechanisms. Given the potential climate change impact discussed in this study, these results also highlight the importance of considering the inclusion of land-use and land-cover change-induced teleconnection processes in detection and attribution of anthropogenic climate change. To date, the contribution of these mechanisms to anthropogenic climate change has been absent in the IPCC assessment reports.

In some ways, the results presented here should not be too surprising. We already believe that tropical heating anomalies linked to changes in sea surface temperature (e.g., El Niño) communicate to the extratropics through teleconnections. Given the strength of deep tropical convection over land, and the importance of deforestation on the energy and water balance, it is not surprising that such a teleconnection can also be induced over land. But detecting such changes in long-term observations will be much more difficult than detecting the teleconnection patterns associated with ENSO. ENSO is a relatively rapid process, leaving a clear, repeating signature in the historical climate record. Tropical deforestation, on the other hand, is happening relatively slowly—and is not switching between alternate states every few years. Nevertheless, it is clear that tropical deforestation could have significant implications for the climate system—both in the tropics and across much of the Northern Hemisphere.

**Acknowledgments.** The author acknowledges constructive input and collaboration with Jonathan Foley and Matthew Hitchman on the research herein and in strengthening the manuscript. Walter Robinson kindly provided valuable input on the dynamical processes and in dissecting the model behavior. The author is indebted to Richard Betts and one anonymous reviewer for their insightful and constructive comments on this manuscript.

## References

- Amthor, J. S., 1984: The role of maintenance respiration in plant growth. *Plant Cell Environ.*, **7**, 561–569.
- Asner, G. P., D. E. Knapp, E. N. Broadbent, P. J. C. Oliveira, M. Keller, and J. N. Silva, 2005: Selective logging in the Brazilian Amazon. *Science*, **310**, 480–482.
- Avissar, R., and D. Werth, 2005: Global hydroclimatological teleconnections resulting from tropical deforestation. *J. Hydrometeor.*, **6**, 134–145.
- Betts, R. A., P. M. Cox, M. Collins, P. P. Harris, C. Huntingford, and C. D. Jones, 2004: The role of ecosystem–atmosphere interactions in simulated Amazonian precipitation decrease and forest dieback under global climate warming. *Theor. Appl. Climatol.*, **78**, 157–175.
- Bonan, G. B., 1995: Land-atmosphere CO<sub>2</sub> exchange simulated by a land surface process model coupled to an atmospheric general circulation model. *J. Geophys. Res.*, **100** (D2), 2817–2831.
- Chase, T. N., R. A. Pielke, T. G. F. Kittel, R. R. Nemani, and S. W. Running, 2000: Simulated impacts of historical land cover changes on global climate in northern winter. *Climate Dyn.*, **16**, 93–105.
- Collatz, G. J., J. T. Ball, C. Grivet, and J. A. Berry, 1991: Physiological and environmental regulation of stomatal conductance, photosynthesis and transpiration: A model that includes a laminar boundary layer. *Agric. For. Meteorol.*, **54**, 107–136.

- , M. Ribas-Carbo, and J. A. Berry, 1992: Coupled photosynthesis–stomatal conductance model for leaves of C4 plants. *Aust. J. Plant Physiol.*, **19**, 519–538.
- Costa, M. H., and J. A. Foley, 2000: Combined effects of deforestation and doubled atmospheric CO<sub>2</sub> concentrations on the climate of Amazonia. *J. Climate*, **13**, 18–34.
- , S. N. M. Yanagi, P. J. O. P. Souza, A. Ribeiro, and E. J. P. Rocha, 2007: Climate change in Amazonia caused by soybean cropland expansion, as compared to caused by pastureland expansion. *Geophys. Res. Lett.*, **34**, L07706, doi:10.1029/2007GL029271.
- Da Silva, R. R., D. Werth, and R. Avissar, 2008: Regional impacts of future land-cover changes on the Amazon basin wet-season climate. *J. Climate*, **21**, 1153–1170.
- Delire, C., P. Behling, M. T. Coe, J. A. Foley, R. Jacob, J. Kutzbach, Z. Y. Liu, and S. Vavrus, 2001: Simulated response of the atmosphere–ocean system to deforestation in the Indonesian Archipelago. *Geophys. Res. Lett.*, **28**, 2081–2084.
- , S. Levis, G. Bonan, J. A. Foley, M. Coe, and S. Vavrus, 2002: Comparison of the climate simulated by the CCM3 coupled to two different land-surface models. *Climate Dyn.*, **19**, 657–669.
- Denman, K. L., and Coauthors, 2007: Couplings between changes in the climate system and biogeochemistry. *Climate Change 2007: The Physical Science Basis*, S. Solomon et al., Eds., Cambridge University Press, 499–588.
- Dickinson, R. E., and A. Henderson-Sellers, 1988: Modelling tropical deforestation: A study of GCM land-surface parametrizations. *Quart. J. Roy. Meteor. Soc.*, **114**, 439–462.
- FAO, 2001: Forest resources assessment 2000. Food and Agricultural Organization, FAO Forestry Paper 140, 511 pp. [Available online at <http://www.fao.org/forestry/fra/2000/report/en/>.]
- Farquhar, G. D., S. V. Caemmerer, and J. A. Berry, 1980: A biochemical model of photosynthetic CO<sub>2</sub> assimilation in leaves of C3 species. *Planta*, **149**, 78–90.
- Findell, K. L., T. R. Knutson, and P. C. D. Milly, 2006: Weak simulated extratropical responses to complete tropical deforestation. *J. Climate*, **19**, 2835–2850.
- Foley, J. A., I. C. Prentice, N. Ramankutty, S. Levis, D. Pollard, S. Sitch, and A. Haxeltine, 1996: An integrated biosphere model of land surface processes, terrestrial carbon balance, and vegetation dynamics. *Global Biogeochem. Cycles*, **10**, 603–628.
- , M. H. Costa, C. Delire, N. Ramankutty, and P. Snyder, 2003: Green surprise? How terrestrial ecosystems could affect earth’s climate. *Front. Ecol. Environ.*, **1**, 38–44.
- , and Coauthors, 2005: Global consequences of land use. *Science*, **309**, 570–574.
- , and Coauthors, 2007: Amazonia revealed: Forest degradation and loss of ecosystem goods and services in the Amazon Basin. *Front. Ecol. Environ.*, **5**, 25–32.
- Gedney, N., and P. J. Valdes, 2000: The effect of Amazonian deforestation on the Northern Hemisphere circulation and climate. *Geophys. Res. Lett.*, **27**, 3053–3056.
- Hahmann, A. N., and R. E. Dickinson, 1997: RCCM2-BATS model over tropical South America: Applications to tropical deforestation. *J. Climate*, **10**, 1944–1964.
- Hasler, N., D. Werth, and R. Avissar, 2009: Effects of tropical deforestation on global hydroclimate: A multimodel ensemble analysis. *J. Climate*, **22**, 1124–1141.
- Hegerl, G. C., and Coauthors, 2007: Understanding and attributing climate change. *Climate Change 2007: The Physical Science Basis*, S. Solomon et al., Eds., Cambridge University Press, 663–746.
- Henderson-Sellers, A., R. E. Dickinson, T. B. Durbidge, P. J. Kennedy, K. Mcguffie, and A. J. Pitman, 1993: Tropical deforestation: Modeling local-scale to regional-scale climate change. *J. Geophys. Res.*, **98** (D4), 7289–7315.
- Hoskins, B. J., and D. J. Karoly, 1981: The steady linear response of a spherical atmosphere to thermal and orographic forcing. *J. Atmos. Sci.*, **38**, 1179–1196.
- IGBP-DIS, cited 2000: Global gridded surfaces of selected soil characteristics (IGBP-DIS). Oak Ridge National Laboratory Distributed Active Archive Center. [Available online at [http://webmap.ornl.gov/wcsdown/dataset.jsp?ds\\_id=569](http://webmap.ornl.gov/wcsdown/dataset.jsp?ds_id=569).]

- Kiehl, J. T., J. J. Hack, G. B. Bonan, B. A. Boville, D. L. Williamson, and P. J. Rasch, 1998: The National Center for Atmospheric Research Community Climate Model: CCM3. *J. Climate*, **11**, 1131–1149.
- Kucharik, C. J., and Coauthors, 2000: Testing the performance of a Dynamic Global Ecosystem Model: Water balance, carbon balance, and vegetation structure. *Global Biogeochem. Cycles*, **14**, 795–825.
- Lean, J., and D. A. Warrilow, 1989: Simulation of the regional climatic impact of Amazon deforestation. *Nature*, **342**, 411–413.
- , and P. R. Rowntree, 1993: A GCM simulation of the impact of Amazonian deforestation on climate using an improved canopy representation. *Quart. J. Roy. Meteor. Soc.*, **119**, 509–530.
- , and —, 1997: Understanding the sensitivity of a GCM simulation of Amazonian deforestation to the specification of vegetation and soil characteristics. *J. Climate*, **10**, 1216–1235.
- Nobre, C. A., P. J. Sellers, and J. Shukla, 1991: Amazonian deforestation and regional climate change. *J. Climate*, **4**, 957–988.
- Pielke, R. A., 2001: Influence of the spatial distribution of vegetation and soils on the prediction of cumulus convective rainfall. *Rev. Geophys.*, **39**, 151–177.
- , G. Marland, R. A. Betts, T. N. Chase, J. L. Eastman, J. O. Niles, D. D. S. Niyogi, and S. W. Running, 2002: The influence of land-use change and landscape dynamics on the climate system: Relevance to climate-change policy beyond the radiative effect of greenhouse gases. *Philos. Trans. Roy. Soc. London*, **A360**, 1705–1719.
- Pitman, A. J., and Coauthors, 2009: Uncertainties in climate responses to past land cover change: First results from the LUCID intercomparison study. *Geophys. Res. Lett.*, **36**, L14814, doi:10.1029/2009GL039076.
- Polcher, J., 1995: Sensitivity of tropical convection to land-surface processes. *J. Atmos. Sci.*, **52**, 3143–3161.
- Ramankutty, N., and J. A. Foley, 1999: Estimating historical changes in global land cover: Croplands from 1700 to 1992. *Global Biogeochem. Cycles*, **13**, 997–1027.
- Sellers, P. J., Y. Mintz, Y. C. Sud, and A. Dalcher, 1986: A Simple Biosphere Model (Sib) for use within general circulation models. *J. Atmos. Sci.*, **43**, 505–531.
- Snyder, P. K., C. Delire, and J. A. Foley, 2004a: Evaluating the influence of different vegetation biomes on the global climate. *Climate Dyn.*, **23**, 279–302.
- , J. A. Foley, M. H. Hitchman, and C. Delire, 2004b: Analyzing the effects of complete tropical forest removal on the regional climate using a detailed three-dimensional energy budget: An application to Africa. *J. Geophys. Res.*, **109**, D21102, doi:10.1029/2003JD004462.
- Sud, Y. C., J. Shukla, and Y. Mintz, 1988: Influence of land surface roughness on atmospheric circulation and precipitation: A sensitivity study with a general circulation model. *J. Appl. Meteor.*, **27**, 1036–1054.
- , G. K. Walker, J.-H. Kim, G. E. Liston, P. J. Sellers, and W. K.-M. Lau, 1996: Biogeophysical consequences of a tropical deforestation scenario: A GCM simulation study. *J. Climate*, **9**, 3225–3247.
- Thompson, D. W. J., and J. M. Wallace, 1998: The Arctic Oscillation signature in the wintertime geopotential height and temperature fields. *Geophys. Res. Lett.*, **25**, 1297–1300.
- , and —, 2000: Annular modes in the extratropical circulation. Part I: Month-to-month variability. *J. Climate*, **13**, 1000–1016.
- Trenberth, K. E., G. W. Branstator, D. Karoly, A. Kumar, N. C. Lau, and C. Ropelewski, 1998: Progress during TOGA in understanding and modeling global teleconnections associated with tropical sea surface temperatures. *J. Geophys. Res.*, **103** (C7), 14 291–14 324.
- Voldoire, A., and J. F. Royer, 2005: Climate sensitivity to tropical land surface changes with coupled versus prescribed SSTs. *Climate Dyn.*, **24**, 843–862.
- Wallace, J. M., and D. S. Gutzler, 1981: Teleconnections in the geopotential height field during the Northern Hemisphere winter. *Mon. Wea. Rev.*, **109**, 784–812.

- Werth, D., and R. Avissar, 2002: The local and global effects of Amazonian deforestation. *J. Geophys. Res.*, **107**, 8087, doi:10.1029/2001JD000717.
- Zhang, H., K. McGuffie, and A. Henderson-Sellers, 1996: Impacts of tropical deforestation. Part II: The role of large-scale dynamics. *J. Climate*, **9**, 2498–2521.
- Zhao, M., A. J. Pitman, and T. Chase, 2001: The impact of land cover change on the atmospheric circulation. *Climate Dyn.*, **17**, 467–477.
- Zwiers, F. W., and H. von Storch, 1995: Taking serial correlation into account in tests of the mean. *J. Climate*, **8**, 336–351.

---

*Earth Interactions* is published jointly by the American Meteorological Society, the American Geophysical Union, and the Association of American Geographers. Permission to use figures, tables, and *brief* excerpts from this journal in scientific and educational works is hereby granted provided that the source is acknowledged. Any use of material in this journal that is determined to be “fair use” under Section 107 or that satisfies the conditions specified in Section 108 of the U.S. Copyright Law (17 USC, as revised by P.L. 94-553) does not require the publishers’ permission. For permission for any other form of copying, contact one of the copublishing societies.

---

Copyright of Earth Interactions is the property of American Meteorological Society and its content may not be copied or emailed to multiple sites or posted to a listserv without the copyright holder's express written permission. However, users may print, download, or email articles for individual use.